



UNIVERSITÀ  
degli STUDI  
di CATANIA

**DOTTORATO DI RICERCA IN BIOMEDICINA TRASLAZIONALE  
XXXVIII CICLO**

COORDINATORE: *PROF. CARLO VANCHERI*

---

*GIULIANO COSTA*

**TRANSCATHETER AORTIC VALVE REPLACEMENT USING  
SELF-EXPANDING VALVES DEPLOYED WITH INTENTIONAL,  
PATIENT-SPECIFIC COMMISSURAL ALIGNMENT:  
THE REACCESS 2 STUDY**

Tesi di Dottorato

Tutor: Prof. D. Capodanno

---

Anno Accademico 2024/2025

*Alla mia famiglia*

# **SUMMARY**

<b>1. INTRODUCTION</b>	<b>5</b>
<b>2. RATIONALE, DEFINITIONS, TECHNIQUES, AND OUTCOMES OF COMMISSURAL ALIGNMENT IN TAVR</b>	<b>7</b>
<b>2.1 Commissural alignment and impact on coronary access</b>	<b>7</b>
<b>2.2 Commissural alignment and impact on valve hemodynamic</b>	<b>9</b>
<b>2.3 Redo-TAVR and coronary access after valve-in-valve procedures</b>	<b>10</b>
<b>2.4 Commissural alignment definitions</b>	<b>11</b>
<b>2.5 Preprocedural planning to achieve commissural alignment</b>	<b>13</b>
<b>2.6 CT-derived fluoroscopic projection</b>	<b>13</b>
<b>2.7 CT-based simulation</b>	<b>16</b>
<b>2.8 Implantation techniques and outcomes with different transcatheter valves</b>	<b>18</b>
<b>2.9 Limitations of the implantation techniques</b>	<b>22</b>
<b>3. CORONARY CANNULATION FOLLOWING TRANSCATHETER AORTIC VALVE REPLACEMENT USING SELF-EXPANDING DEVICES WITH COMMISSURAL ALIGNMENT</b>	<b>23</b>
<b>3.1 Introduction</b>	<b>23</b>
<b>3.2 Methods</b>	<b>24</b>
<b>3.3 Results</b>	<b>28</b>
<b>3.4 Discussion</b>	<b>44</b>

<b>3.5 Limitations</b>	<b>49</b>
<b>4. <i>TRANSCATHETER HEART VALVE FRAME DINAMICITY ACROSS THE CARDIAC CYCLE AFTER TRANSCATHETER AORTIC VALVE REPLACEMENT WITH COMMISSURAL ALIGNMENT</i></b>	<b>50</b>
<b>4.1 Introduction</b>	<b>50</b>
<b>4.2 Methods</b>	<b>51</b>
<b>4.3 Results</b>	<b>55</b>
<b>4.4 Discussion</b>	<b>62</b>
<b>4.5 Limitations</b>	<b>64</b>
<b>5. <i>CONCLUSIONS</i></b>	<b>65</b>
<b>6. <i>REFERENCES</i></b>	<b>66</b>

## 1. INTRODUCTION

As transcatheter aortic valve replacement (TAVR) expands to younger, low-risk patients with longer life expectancies, lifetime management of their cardiovascular disease, such as the need for future interventions for valve dysfunction and/or coronary artery disease, is becoming increasingly important (1,2).

Although the incidence of coronary access after TAVR currently remains low, given the prevalence of coronary artery disease in low- to high-risk patients ranging from >20% to >50%, it will likely increase as TAVR becomes the preferred therapy in aortic stenosis (3).

Unlike surgical aortic valve replacement (SAVR), which places commissural posts in alignment with the native aortic valve commissures and away from coronary ostia, in TAVR there have been no commercially available devices or techniques to consistently achieve commissural alignment. Recent literature has shown that commissural posts of transcatheter heart valves (THVs), when facing a coronary orifice, may create a physical barrier, making coronary access more challenging (3).

In addition, as redo-TAVR is being considered for THV failure, having commissural misalignment will impact the feasibility of the procedure given the risk of sinus sequestration and coronary obstruction as well as the inability to consider leaflet modification techniques to mitigate against these risks.

Finally, THV commissural alignment (CA) may play a role in maintaining a physiological blood flow within the aortic root, and therefore in preserve bioprosthetic leaflet functioning and valve durability at long-term (**Figure 1**).

During this PhD, the candidate conducted a prospective, single-center study to evaluate the feasibility of re-engaging the coronary ostia after TAVR using self-expanding THVs implanted aiming at CA, to discover potential native anatomic or prosthesis-related features that may preclude optimal coronary re-access after TAVR, and to assess in-vivo THV frame behavior during the cardiac cycle using post-TAVR 4-dimensional (4D-CTA).

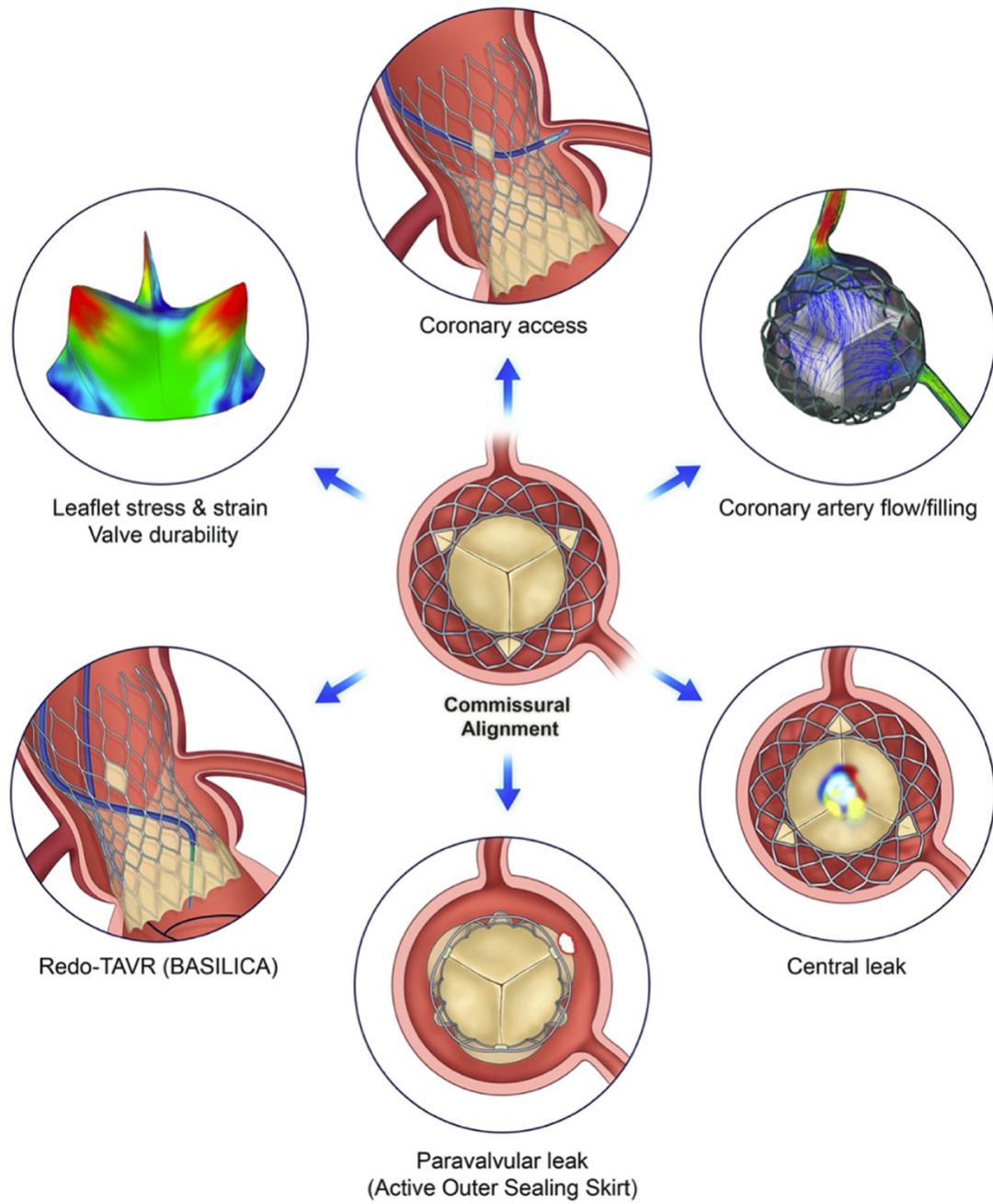


**Figure 1.** Possible impact of commissural alignment in transcatheter aortic valve replacement therapy

## **2. RATIONALE, DEFINITIONS, TECHNIQUES, AND OUTCOMES OF COMMISSURAL ALIGNMENT IN TAVR**

### **2.1 Commissural alignment and impact on coronary access**

Commissural alignment is defined according to the angular relationship between native and bioprosthetic valve commissures. The degree of commissural misalignment correlates to the risk of overlap between neo-commissures and native coronary ostia. Fuchs and colleagues first evaluated the issue of commissural misalignment in patients undergoing TAVR, reporting a strict alignment of neo-commissures in only about 20% of patients(4). Despite isolated case series and retrospective studies having shown that coronary access after TAVR was mostly feasible, recent data suggest that coronary cannulation can be impaired in a significant portion of patients. The RE-ACCESS (Reobtain Coronary Ostia Cannulation Beyond Transcatheter Aortic Valve Stent) study was the first prospective investigation on this issue. In this analysis, selective coronary re-engagement was unsuccessful in 7.7% of cases after TAVR. The use of self-expanding supra-annular THVs (Evolut R/PRO, Medtronic Inc), device implant depth, and THVs oversized with respect to the sinus of Valsalva diameter were independent predictors of un-successful coronary cannulation (5).

With TAVR, commissural posts may impede coronary access, and, until recently, THV orientations were deemed random and not predictable during valve deployment, a potential drawback compared with the surgical bioprostheses with which surgeons can achieve commissural alignment during SAVR and coronary access afterward is straightforward. THV design also influences coronary re-engagement after TAVR; a shorter stent frame height and larger cell design ensure an easier access to coronary

arteries, and an intra-annular position of bioprosthetic leaflets respects native anatomy and more likely maintains the anatomic configuration of the aortic root (6–8).

Fluoroscopic markers on the THV commissural posts may also make coronary access potentially easier by helping visualize the proximity of the commissural post to the coronary ostium.

A post-implantation computed tomography (CT) analysis showed that the incidence of CT features of unfavourable coronary access (ie, the coronary ostium located below the skirt or in front of the THV commissural posts above the skirt) occurred more frequently in the Evolut R/PRO group than the SAPIEN 3 (Edwards Lifesciences) group (22.7% vs 11.3% for the left main coronary artery; 21.2% vs 8.1% for the right coronary artery) (9). This study highlighted the impact of different leaflet positions and heights on the coronary access.

The Evolut THV, whose leaflets are sutured in a supra-annular position, has commissural posts that extend up to 26 mm above the inflow edge of the valve; this results in a large, triangle-shaped area covered by the leaflet tissue and creates a physical barrier to coronary access.

This same issue may also involve other self-expanding THVs with high commissural posts (eg, ACURATE Neo2, Boston Scientific). In general, THVs with high commissural posts are intended to reduce leaflet stress and potentially improve durability but do impact coronary access. On the other hand, the SAPIEN 3 Ultra valve (Edwards Lifesciences) and the Portico/Navitor (Abbott Structural Heart) have an intra-annular leaflet position, creating less of a barrier when it comes to coronary access.

A similar rate of patients receiving SAPIEN 3 and having unfavourable characteristics for coronary access (including the SAPIEN 3 frame above and a commissural post in front of the coronary ostium) was reported in the MedStar low-risk trial (10). However, in the RE-ACCESS study, the risk of the inability for coronary access after TAVR with balloon-expandable THVs and the self-expanding Portico/Navitor remained lower than the self-

expanding supra-annular Evolut THV(5). However, the ALIGN-ACCESS (TAVR With Commissural Alignment Followed by Coronary Access) study investigated the impact of commissural alignment on the feasibility of coronary access after TAVR and showed that commissural alignment of supra-annular THVs with native commissures improves the feasibility of selective coronary angiography after TAVR (11).

In case of challenging anatomy for coronary access, using advanced coronary techniques may solve the issue (12). Still, these strategies ensuring correct coronary access might increase the procedural duration, contrast administration, and the risk of complications in cases of complex percutaneous coronary intervention.

## **2.2 Commissural alignment and impact on valve hemodynamic**

In addition to impacting coronary access, commissural misalignment has been associated with changes in the fluid flow patterns, increasing leaflet stress, and creating non-physiological vorticity that can result in an increased blood stagnation inside the sinus of Valsalva (13,14). This mechanism may promote pathological scenarios, such as increased thrombogenicity of blood flow and plaque formation, potentially leading to early valve degeneration. In an in vitro study, compared with commissural alignment, misalignment in SAPIEN XT THV (Edwards Lifesciences) was not associated with differences in valve hydrodynamic performance, but there were alterations in fluid flow patterns (13). The increased risk of subclinical leaflet thrombosis and potential earlier degeneration of a balloon-expandable THV with commissural misalignment remains hypothetical. Recently, a 40% incidence of hypo-attenuated leaflet thickening in SAPIEN 3 TAVR with commissural misalignment versus 28% with commissural alignment was reported (15). The association of hypo-attenuated leaflet thickening with commissural misalignment and the impact on THV durability requires further investigation and may become clinically important in younger patients.

In terms of hemodynamic performance, commissural misalignment has been shown in the RESOLVE (Assessment of TRanscathetER and Surgical Aortic BiOprosthetic Valve Thrombosis and Its TrEatment With Anticoagulation) registry to be independently associated with a relative aortic valve mean gradient increase of >50% from baseline to 30 days (16). However, data about the importance of this phenomenon remain scarce, and larger and longer-term studies are needed to better understand this issue and its clinical relevance. In addition, THVs implanted with moderate or severe commissural misalignment had been associated with a significantly higher rate of mild transvalvular aortic regurgitation. One hypothesis might be linked to less efficient bioprosthetic leaflet closure during early diastole, which may occur in case of significant commissural misalignment.

### **2.3 Redo-TAVR and coronary access after valve-in-valve procedures**

Commissural misalignment plays an important role regarding the risk of blood flow sequestration within the sinus of Valsalva and coronary access impairment after valve-in-valve procedures. When commissural alignment occurs with the first THV, leaflet modification such as balloon-assisted bioprosthetic aortic scallop intentional laceration to prevent iatrogenic coronary artery obstruction has been shown to be effective for avoiding coronary occlusion before redo-TAVR (17). However, if neo-commissures of the degenerated THV are misaligned, leaflet modification will not be effective (18). Similarly, a THV commissural post facing one of the coronary ostia represents a significant obstacle for coronary access after redo-TAVR, especially if the leaflets have an attachment in the stent frame that is higher than the coronary ostia height (19). A recent CT study of patients undergoing redo-TAVR using the SAPIEN 3 or Evolut THV showed that the use of the SAPIEN 3 as the first valve was associated with more favourable coronary access (20–22). However, even with balloon-expandable valves, the rate of coronary access feasibility

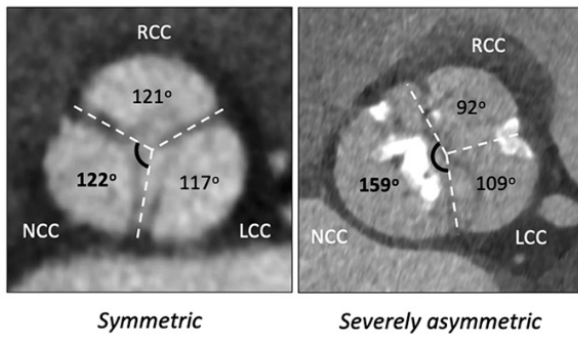
was as low as 68.1% with impossible coronary access ranging between 10% and 27%. The latter was more than twice for Evolut R/Pro valves.

In cases in which the SAPIEN 3 was used first, a higher sino-tubular junction and a THV-to- sino-tubular junction distance  $>2$  mm, were found to be protective against coronary access impairment after redo-TAVR with the same valve (10,23). In cases of a high sino-tubular junction and large aortic root, the shorter frame of the intra-annular SAPIEN 3 valve will ensure a free remaining space between the top of the leaflets and the sino-tubular junction, avoiding the need to snorkel down to the sinus of Valsalva space and coronary artery. Recently, an algorithm has been proposed on TAVR versus SAVR at the index aortic valve intervention based on the sino-tubular junction anatomy to evaluate the possibility of coronary access after redo-TAVR (24). In younger patients with a narrow sino-tubular junction where redo-TAVR may not be feasible because of sinus sequestration, having SAVR as the index procedure followed by TAVR in failed SAVR may reduce the risk of coronary obstruction and better preserve coronary access.

#### **2.4 Commissural alignment definitions**

Commissures are commonly considered aligned if they are within 0 and 15 of each other. Commissural misalignment is graded according to deviations from the native commissures in mild (from 15.1 -30.0°), moderate (from 30.1 -45.0°), and severe (from 45.1 - 60.0°), with coronary overlap defined as an angular distance from one of the commissural posts to a coronary ostium  $<15.0^\circ$  (**Figure 2**) (25).

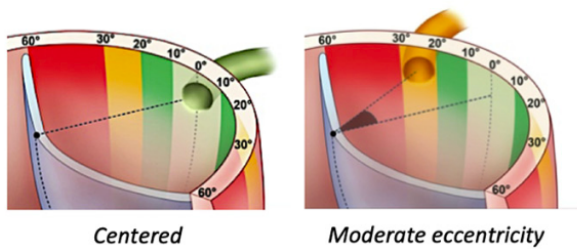
## A AV CUSP SYMMETRY



### Inter-commissural angle of the largest cusp

120.0°-125.0°	symmetric
125.1°-130.0°	mildly asymmetric
130.1°-135.0°	moderately asymmetric
>135.0°	severely asymmetric

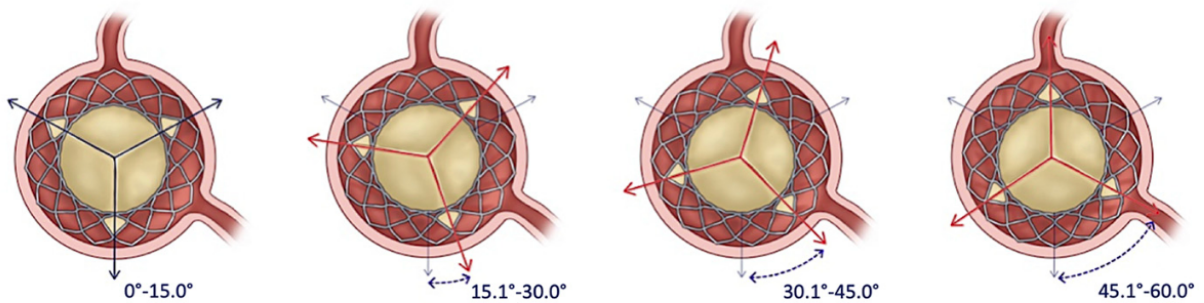
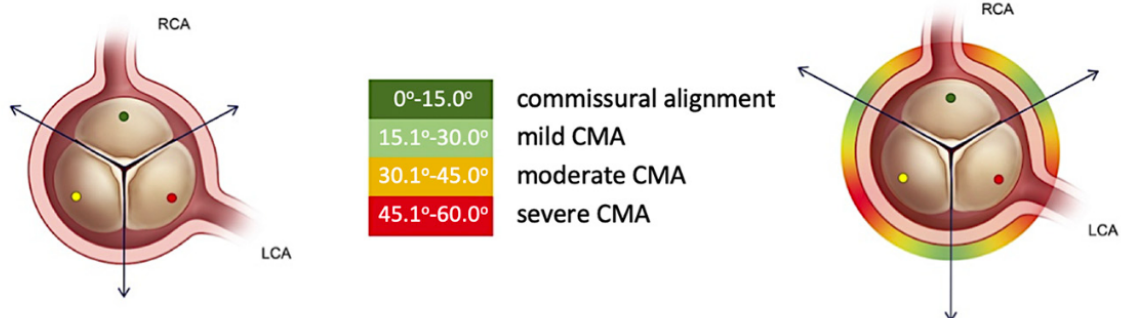
## B CORONARY OSTIAL ECCENTRICITY



### Angle between center-cusp and coronary ostium

0°-10.0°	centered
10.1°-20.0°	mild eccentricity
20.1°-30.0°	moderate eccentricity
>30.0°	severe eccentricity

## C COMMISSURAL (MIS)ALIGNMENT



Commissural alignment

Mild CMA

Moderate CMA

Severe CMA

**Figure 2.** Standardized definitions from the ALIGN-TAVR Consortium.  $V^{1/4}$  aortic valve;  $CMA^{1/4}$  commissural alignment; LCA: left coronary artery; LCC: left coronary cusp;  $NCC^{1/4}$  noncoronary cusp; RCA: right coronary artery; RCC: right coronary cusp; TAVR: transcatheter aortic valve replacement.

## **2.5 Preprocedural planning to achieve commissural alignment**

CT analysis represents an essential step in the pre-procedural planning to identify patient-specific fluoroscopic projections to aim for and evaluate commissural alignment. It allows the operators to select the optimal C-arm angulation to minimize the parallax of the THV frame and the need for repeated pre-deployment contrast injections during the procedure. More recently, additional anatomic information from CT analysis regarding the coronary cusps, the native commissures, and the coronary ostia orientation have become useful landmarks to facilitate patient-specific commissural alignment of TAVR devices. Strategies for CT-based commissural alignment can be classified as: 1) those aiming for patient-specific commissural alignment by identifying a specific fluoroscopic projection adequate for THV implantation and 2) those aiming for a general near-commissural alignment by predicting the TAVR system axial rotation. These approaches are described in the following sections.

## **2.6 CT-derived fluoroscopic projection**

When coronary cusps are symmetrical, each commissure is located at approximately 120° to each other and in front of the opposite coronary cusp. This concept can be used to identify the commissure's location in the CT-derived fluoroscopy angulations (**Figure 3**).

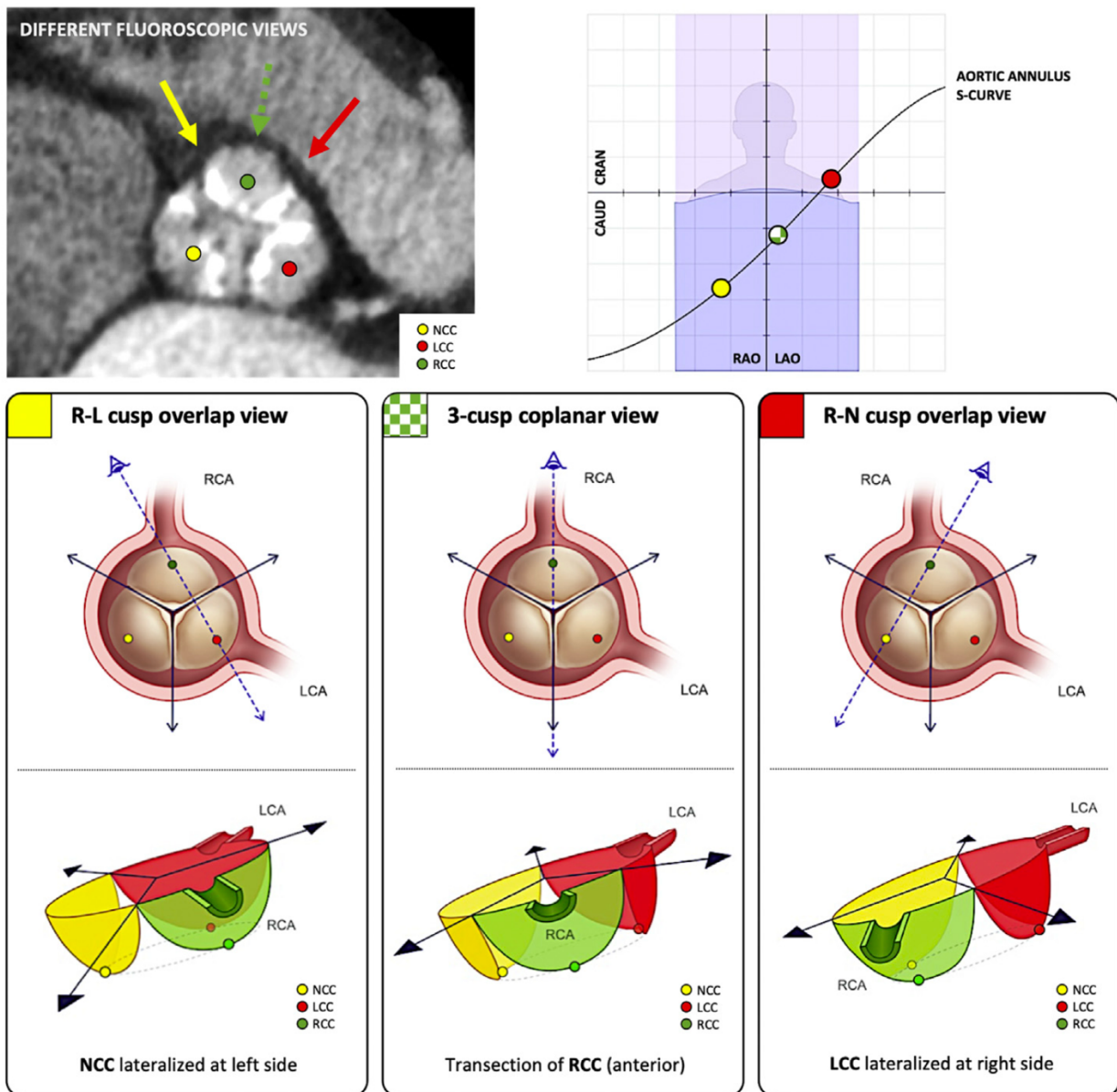


**Figure 3.** Aortic valve cusps and commissural orientation in different computed tomography-derived fluoroscopic views. AV: aortic valve; CAUD: caudal; CRAN: cranial; CT: computed tomography; LAO: left anterior oblique; RAO: right anterior oblique; R-L: right-left; R-N: right-non; other abbreviations as in Figure 2.

In the right coronary cusp (RCC) and the left coronary cusp (LCC) overlap view (usually right anterior oblique [RAO] caudal [CAU]), the noncoronary cusp (NCC) is isolated on the left side of the fluoroscopic screen, and simultaneously the LCC to the RCC commissure is located on the right side (26). Another possible cusp overlap view is the RCC and NCC cusp overlap. This cusp overlap view (usually left anterior oblique cranial) isolates the LCC on the right side of the fluoroscopic screen and the RCC to NCC commissure on the left side.

Finally, in a 3-cusp coplanar view, the RCC is located centered front, and the NCC and LCC commissures are located on either side adjacent to the RCC. This information may allow to align one of the prosthetic commissural posts with the isolated native commissure as an anatomic target that can be verified in several projections. Fluoroscopic markers of commissural posts among different THVs are shown in **Figure 4**.

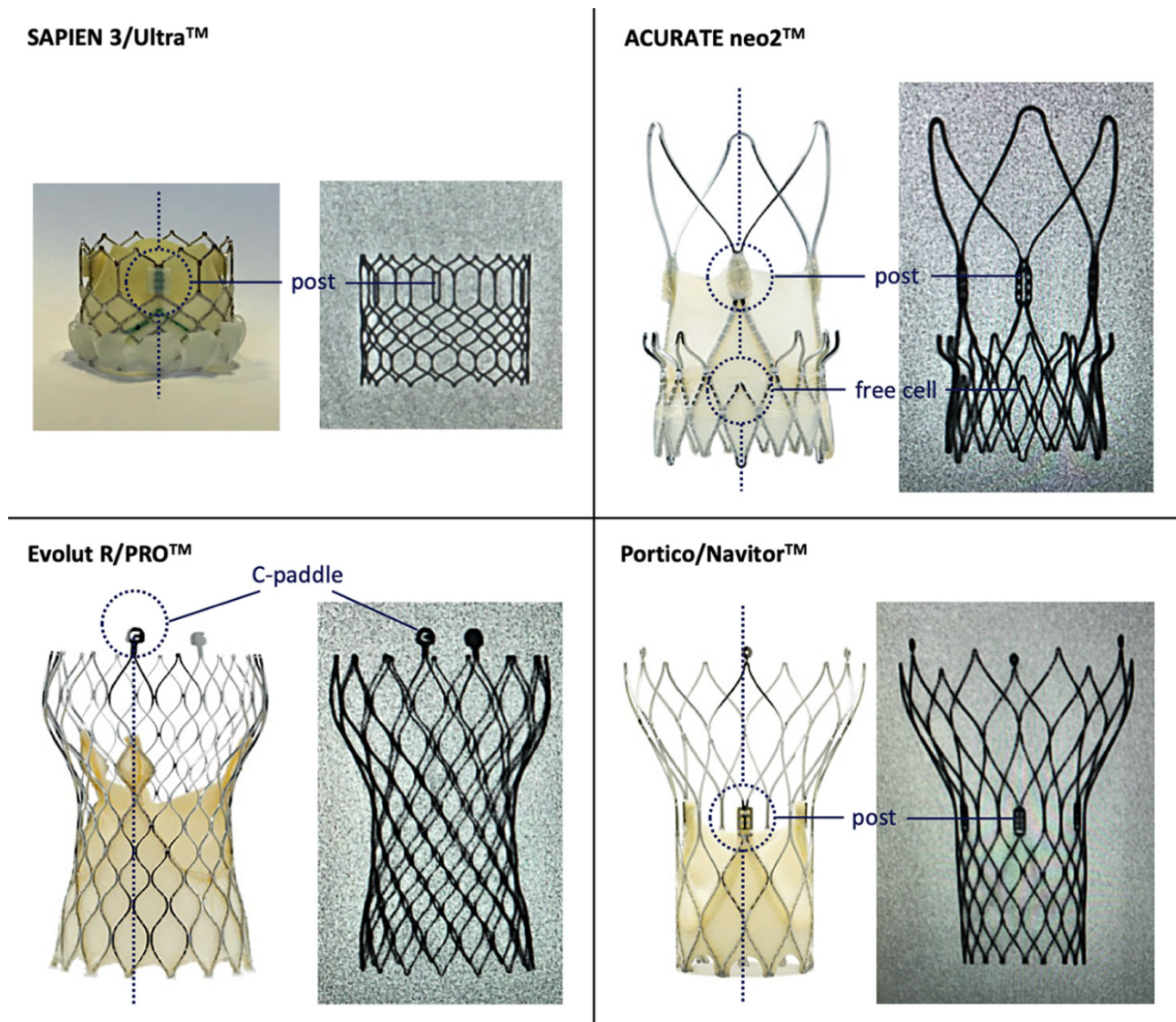


**Figure 4.** Transcatheter heart valve (THV) fluoroscopic markers corresponding with the THV commissures.

## 2.7 CT-based simulation

CT can predict the trajectory of the TAVR devices and their relation to the native commissures and coronary arteries. The Accurate Commissural Alignment project described a CT-based strategy in 11 cases of ACURATE Neo2 implants (27). Controlled commissural alignment was achieved in 3D-dimensional printed in vitro simulation by planning a patient-specific rotation of the delivery system before advancing it within the vascular anatomy (**Figure 5**). The delivery catheter was then advanced into the patient with the recommended orientation, which was maintained throughout the entire procedure. The main advantage of this method is that the rotation of the device inside of the patient is avoided. However, some theoretical concerns arise regarding how tortuous anatomies as well as the spatial orientation of the aortic annular plane may affect the ability of this simplified model to reflect the real trajectory of the delivery catheter from the femoral artery to the aortic annulus. This strategy is also based on 2 assumptions: 1) the aortic centerline is representative of the trajectory of the TAVR device during the deployment; and 2) the THV remains perpendicular to the aortic centerline when it is advanced through the vasculature. Finally, this method remains labor and resource intensive and not practical in routine clinical application because it has not been implemented in imaging software used for TAVR preprocedural planning yet.

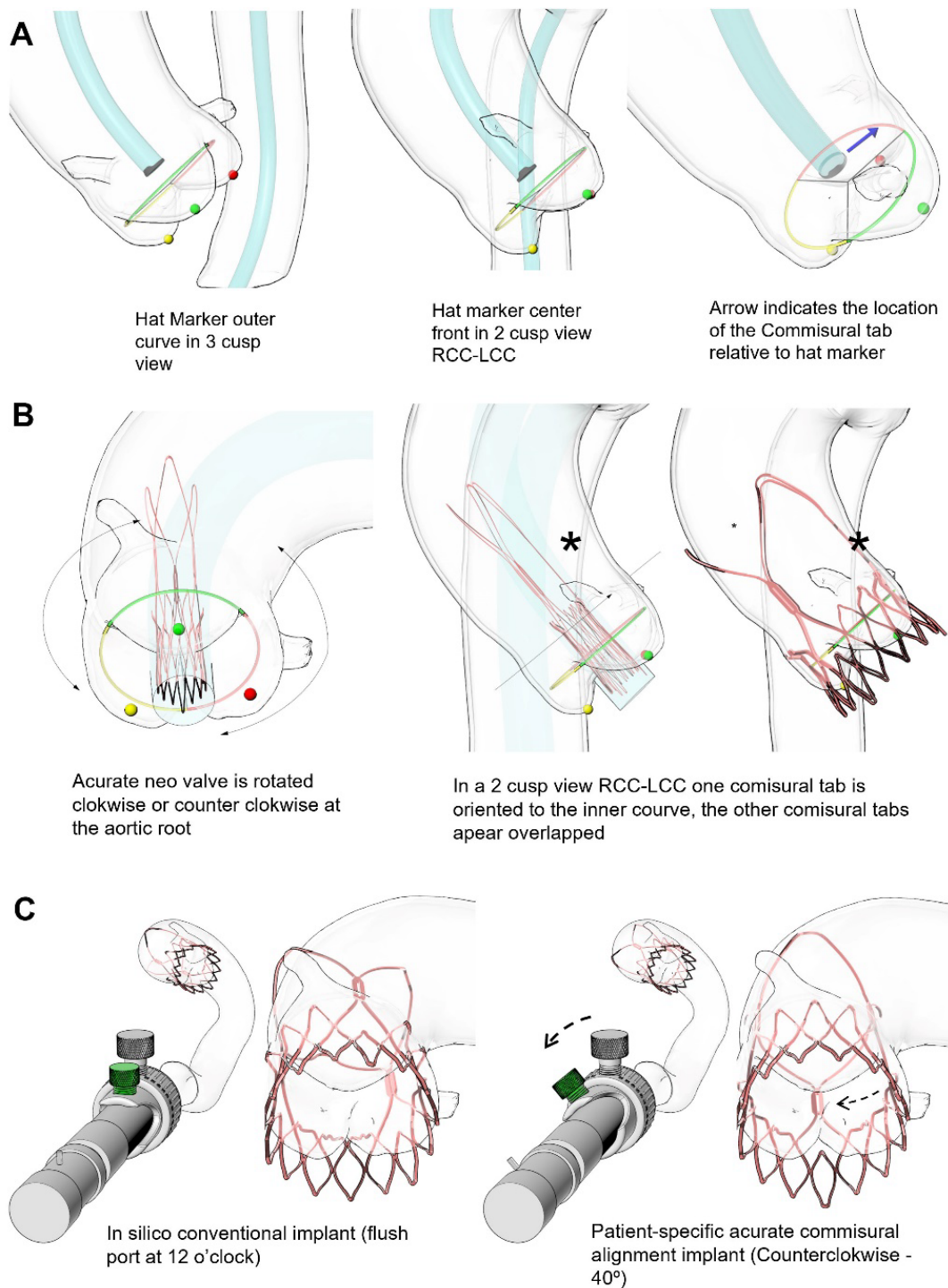


**Figure 5.** Strategies for commissural alignment based on fluoroscopic projection or prediction of TAVR system axial rotation. Orientation of the commissures in the Evolut crimped device based on angiographic projections (A). Orientation of the commissures in the ACURATE Neo2 crimped device based on angiographic projections (B). Patient-specific ACURATE Neo2 implantation with commissural alignment based on predicted rotation by computed tomography analysis (C)

## **2.8 Implantation techniques and outcomes with different transcatheter valves**

### **EVOLUT THV**

The Evolut THV has a C-paddle located at 1 of the commissures and is mounted 90° clockwise from the fluoroscopic “Hat” marker. By inserting the delivery catheter with the flush port at 3 o’clock (away from the operator), the “Hat” marker can be better oriented to the center front at the cusp overlap view during valve implantation, thus optimizing commissural alignment(28–30) (**Figure 6**). With successful commissural alignment, the C-paddle should end up at the inner curve of the ascending aorta at either the 3-cusp or cusp overlap view. When comparing 121 patients who had the conventional 12 o’clock insertion technique with 378 patients who had the 3 o’clock insertion technique, it was found that the incidence of the “Hat” marker at the center front increased significantly from 70.2% to 97.4% ( $p < 0.0001$ ) at the time of deployment. This improved commissural alignment (C-paddle at inner curve) to 80.4% and resulted in a significant reduction in the incidence of severe coronary overlap with Evolut commissure with the left main coronary artery (31.4%-14.3%,  $p < 0.0001$ ), the right coronary artery (20.7%-14.3%,  $p = 0.11$ ), both coronaries (14.0%-5.3%,  $p = 0.0025$ ), or 1 or both coronaries (38.0%-23.3%,  $p = 0.0021$ ). However, given that there are 2 spines within the Evolut delivery catheter, it is not recommended to torque the delivery catheter to improve “Hat” marker position commissural alignment once it is inside the patient because this may potentially damage the delivery system. The new Evolut FX system, with depth markers aligned with the commissures and only 1 spine present, may improve torquability and commissural alignment pending further investigation.

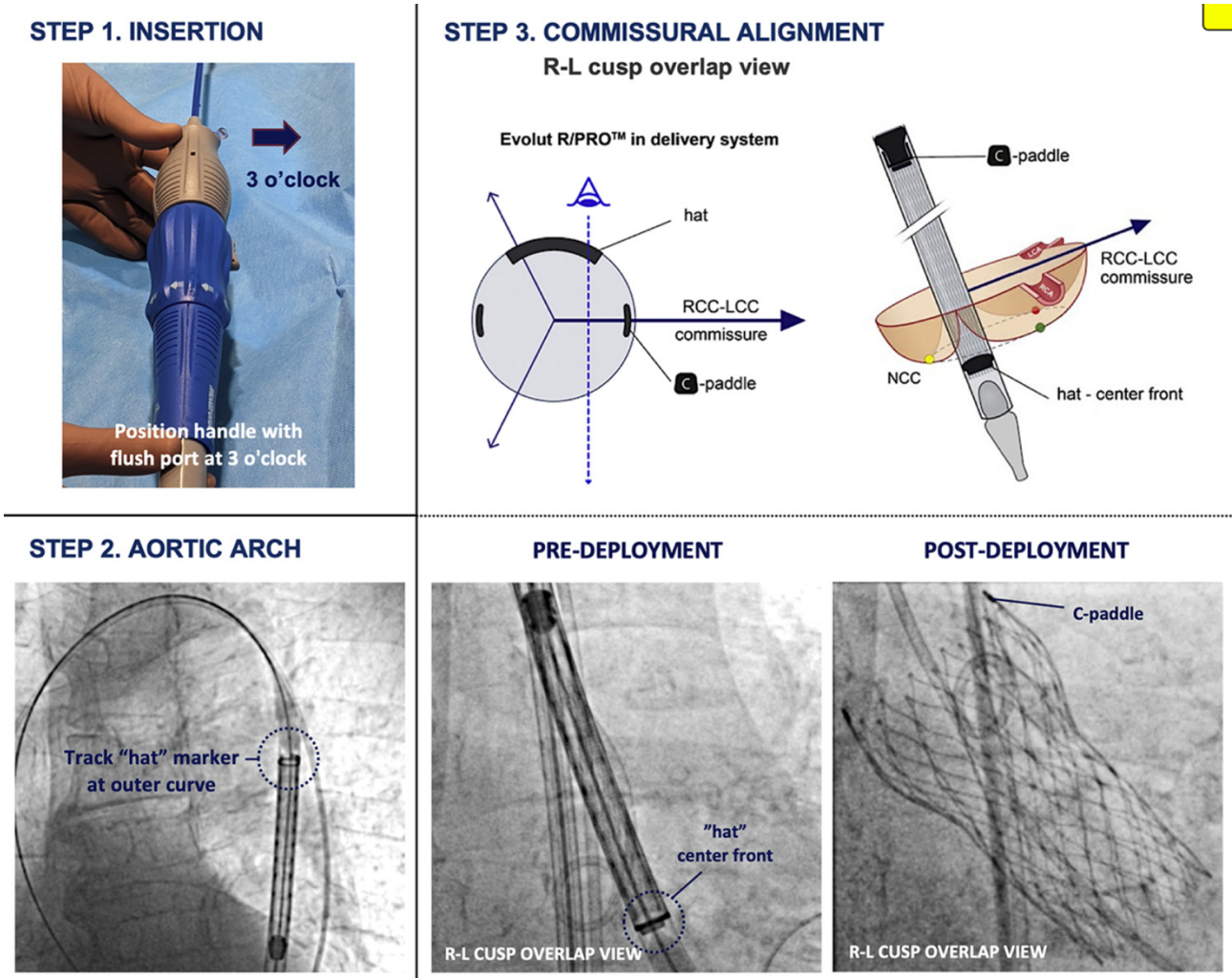


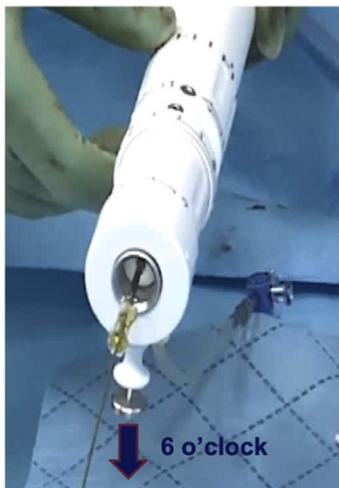
**Figure 6.** Evolut commissural alignment steps. Abbreviations as in Figure 3

## ACURATE Neo2 THV

The ACURATE Neo2 valve is a self-expanding THV with supra-annular leaflet position. The commissures of the ACURATE Neo2 valve can be identified on fluoroscopy by the presence of 3 commissural posts at the base of the stabilizing arches and 3 “free cells” at the level of the upper crown (**Figure 7**). Consequently, the direction of the THV commissures can be easily assessed during valve deployment. The delivery system is flexible and allows rotation of the THV delivery system to more than 60°. In order to implant the ACURATE Neo2 valve with commissural alignment, the following well-defined implantation sequence should be followed. First, insert the delivery system with the flush port facing 6 o’clock, as

operators have reported, to avoid  $\geq$ moderate commissural misalignment in 100% of cases using this method only (26).

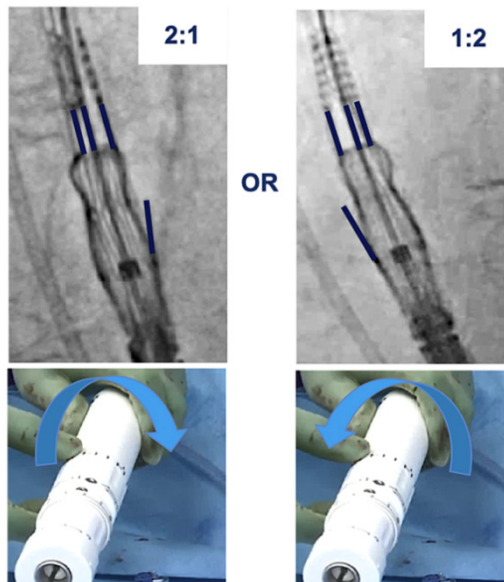
### STEP 1. INSERTION



Position handle with safety button facing down (6 o'clock)

### STEP 2. ASSESS ORIENTATION

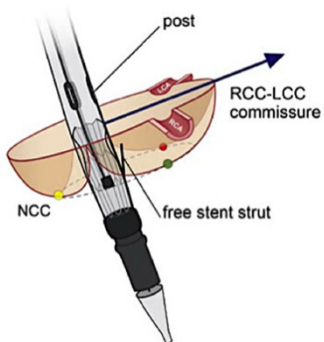
3-cusp coplanar view



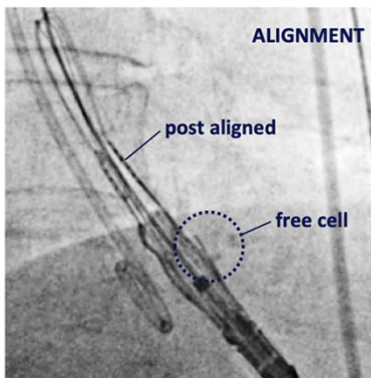
Directionality assessment in 3-cusp coplanar view to minimize rotation to achieve alignment

### STEP 3. ALIGNMENT (ROTATION)

R-L cusp overlap view

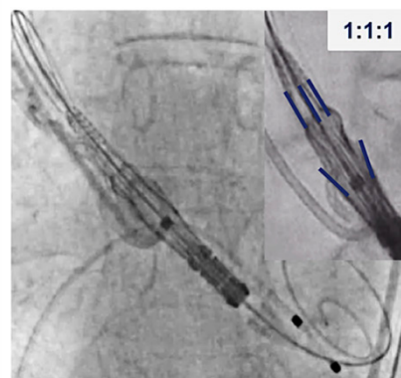


Using directionality, slowly rotate front part of the handle to achieve alignment --- typically 0.5 to 1.0 handle rotations (180° to 360°).



### STEP 4. THV IMPLANT

3-cusp coplanar view



Proceed with classical ACURATE neo2 implantation steps

**Figure 7.** ACURATE Neo2 commissural alignment steps. CCW: counter-clockwise; CW: clockwise; other abbreviations as in Figures 2 to 4.

Second, in order to obtain patient-specific commissural alignment, the ACURATE Neo2 valve should be crossed across the aortic arch, and its orientation should be fine-tuned when the THV is positioned just above the native aortic annulus. The recommended height to rotate the ACURATE Neo2 is when the radiopaque marker is 5 to 10 mm above the aortic annulus (ie, the radiopaque marker at the top of the pigtail catheter).

Third, to make a judgment on the preferred “directionality” to torque the delivery catheter (clockwise or counter-clockwise), the operator should assess the ACURATE Neo2 commissural post configuration in a 3-cusp coplanar view. In case of a 2-1 configuration of the commissural posts, a clockwise rotation of the handle on the delivery catheter is recommended. In case of a 1-2 configuration, a counter-clockwise rotation is recommended. In case of a 1-1-1 configuration, the ACURATE Neo2 is either aligned with the native commissures or has severe commissural misalignment; this will be unmasked in the next verification step. Importantly, one does not torque the delivery catheter yet in this fluoroscopic view.

Fourth, the operator changes the fluoroscopic view to the right-left cusp overlap view and can start optimizing commissural alignment by torquing the delivery catheter (counter)-clockwise. The goal is to rotate the ACURATE Neo2 until 1 of the commissural posts and 1 of the “free cells” is isolated at the right-hand side on the fluoroscopic screen and, hence, is aligned with the native RCC-LCC commissure. In most cases, the initial 90 to 180 torque of the handle will not result in THV rotation at the annulus level. Typically, some torque must be built up in the delivery catheter, and 180 to 360 torque of the handle is needed to rotate the ACURATE Neo2 to the desired orientation. After obtaining a 2-1 commissural post configuration with 1 visible “free cell” at the right-hand side on fluoroscopy, the operator should release his or her hand from the handle and allow spontaneous “spin-back” from the handle, which clears the “overtorque” in the delivery catheter and avoids further unwanted THV rotation when performing the final valve implantation.

Finally, the operator returns to the 3-cusp coplanar view, can verify commissural alignment by checking for a 1-1-1 commissural post configuration, and can continue with valve implantation in the standard fashion. The radiopaque marker is advanced until just above the aortic annulus, and the ACURATE Neo2 valve is implanted by the top-down, 2-step deployment mechanism. The success of the final implant with regard to patient-specific commissural alignment can be easily assessed in the right-left cusp overlap view (31).

## **2.9 Limitations of the implantation techniques**

Limitations may be observed with the previously described implantation techniques to achieve commissural alignment. First, alternate access approaches have not been studied. Second, iliofemoral tortuosity and calcified vascular anatomy may limit the ability to torque or rotate the delivery catheter to achieve alignment during valve deployment. Finally, torquing manoeuvres of the delivery catheters to obtain commissural alignment can potentially increase the risk of embolic events, vascular complications, and damage to the delivery system. Even though commissural alignment is desirable for any TAVR procedure, this should be balanced against the potential complications caused by increased catheter and device manipulation. Further benchtop and larger clinical studies will be necessary to validate the safety and efficacy of intentional annular or aortic rotation of delivery catheters during THV deployment to optimize commissural alignment.

### **3. CORONARY CANNULATION FOLLOWING TAVR USING SELF-EXPANDING DEVICES WITH COMMISSURAL ALIGNMENT**

#### **3.1 Introduction**

Ensuring optimal coronary re-access after TAVR has gained increasing significance in TAVR therapy (6). The progressive decrease in the age of TAVR patients, coupled with the frequent coexistence of severe aortic stenosis and coronary artery disease, underscores the rising importance of facilitating future coronary angiography and percutaneous coronary intervention during the post-procedure follow-up period (32,33). Studies have indicated that small-cells, supra-annular THVs are more prone to impaired coronary re-access as compared to shorter-frame, intra-annular THVs, even though CA techniques for self-expanding valves seem to mitigate this phenomenon. The ALIGN-ACCESS was the sole study that assessed the feasibility of coronary cannulation with coronary angiography after TAVR looking at commissure alignment with the native aortic valve (11). However, intentional CA was not systematically attempted in all patients enrolled in the study and the assessment relied only on fluoroscopy, lacking the integration of computed tomography angiography (CTA).

The principal aim of this prospective, investigator-initiated study was to assess the feasibility to reengage the coronary ostia after TAVR using self-expanding THVs implanted aiming at CA and to discover potential native anatomic or prosthesis-related features that may preclude optimal coronary re-access after TAVR, using post-TAVR CTA.

## **3.2 Methods**

### **Study design**

The RE-ACCESS (Reobtain Coronary Ostia Cannulation Beyond Transcatheter Aortic Valve Stent) 2 study was an investigator-driven, single-center, prospective, registry-based study that used the TAVR institutional registry of Azienda Ospedaliero-Universitaria Policlinico “G. Rodolico-San Marco” in Catania, Italy (REPLACE [Registry of Percutaneous Aortic Valve Replacement]), as the platform for data collection and follow-up assessment. All study management activities, including data management and statistical analyses, were performed at the Division of Cardiology. All subjects provided written informed consent for the procedure and the CTA. The study was conducted according to the principles of the Declaration of Helsinki and Good Clinical Practice, and approved by the local institutional review board. The authors wrote all drafts of the paper and vouch for the integrity of and completeness of the data and analyses. Details of the REPLACE Registry has been previously reported(34).

### **Study Population**

All consecutive patients with severe aortic stenosis of the native valve undergoing TAVR utilizing the Evolut R, PRO and PRO+ (Medtronic Inc) and the ACURATE Neo 2 (Boston Scientific) devices, implanted using procedural techniques aimed at achieving CA and with baseline cardiac electrocardiographically gated CTA examinations were considered eligible for the study. Exclusion criteria were: 1) the presence of a degenerated aortic bioprosthesis; 2) known coronary ostial chronic total occlusion; 3) native bicuspid aortic valve; 4) device failure; 5) hemodynamic instability during the procedure; 6) stage IV/V chronic kidney injury. Study participant flow is reported in **Figure 8**.

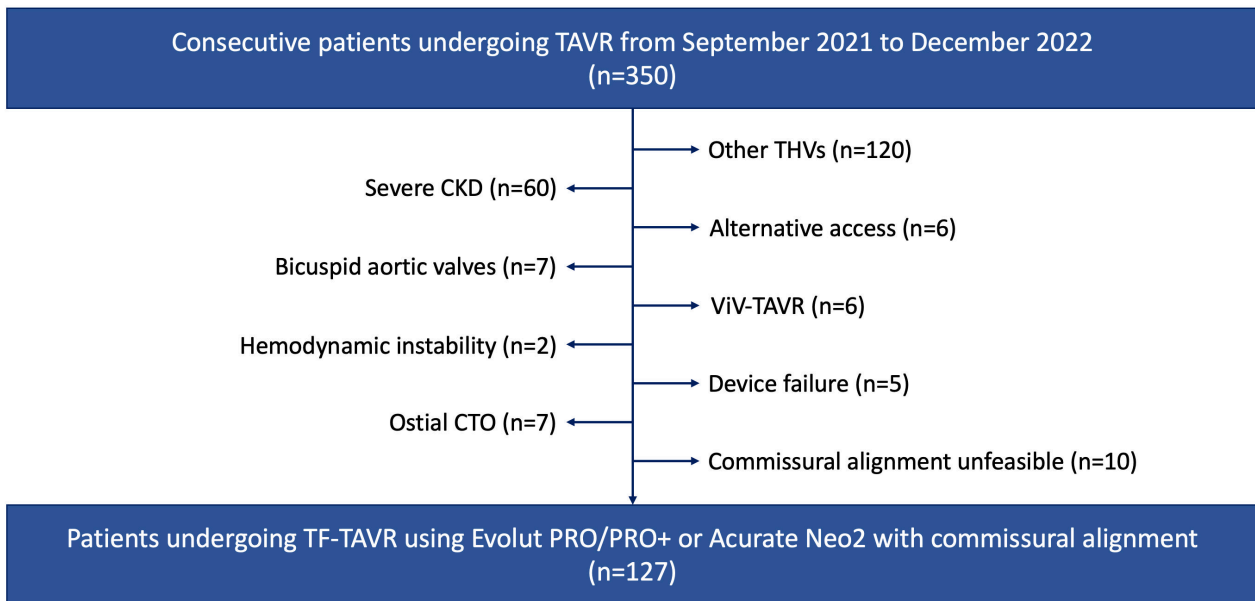


**Figure 8.** Study participant flow

## Study Procedure

Commissure alignment was attempted using the current recommendations described ALIGN-TAVR Consortium (25). In details, the “3-cusp” and “cusp-overlap” views were generated by the baseline CTA assessment. For the Evolut THV, the delivery catheter was inserted with the flush port at 3 o’clock; if necessary, the “Hat” marker was better oriented to the center front at the cusp overlap view during valve implantation, to optimize CA. For the ACURATE Neo 2 THV, the delivery system was inserted with the flush port facing 6 o’clock. If necessary, when the radiopaque marker of the ACURATE Neo 2 was 5 to 10 mm above the aortic annulus, fine-tuning adjustment (clockwise or counterclockwise rotation) was applied to optimize the alignment.

As per study protocol, left and right coronary angiography was performed in each patient after TAVR through a transfemoral approach. Two expert operators performed coronary angiography after TAVR (M.B. and G.C.). Types of catheters used, timing of cannulation, and amount of contrast media administered were collected. The choice of catheters and techniques for coronary cannulation after TAVR were left to the discretion of the operator.

## CTA assessment pre- and after TAVR

All CTA examinations were evaluated by 3 cardiac computed tomography readers (M.B., G.C. and V.G.). The assessment of the baseline CTA was previously described (5). For the post-TAVR CTA assessment, the key measurements are illustrated in **Figure 9**. The implantation depth was obtained by measuring perpendicularly from the nadir of each coronary sinus to the THV inflow plane.

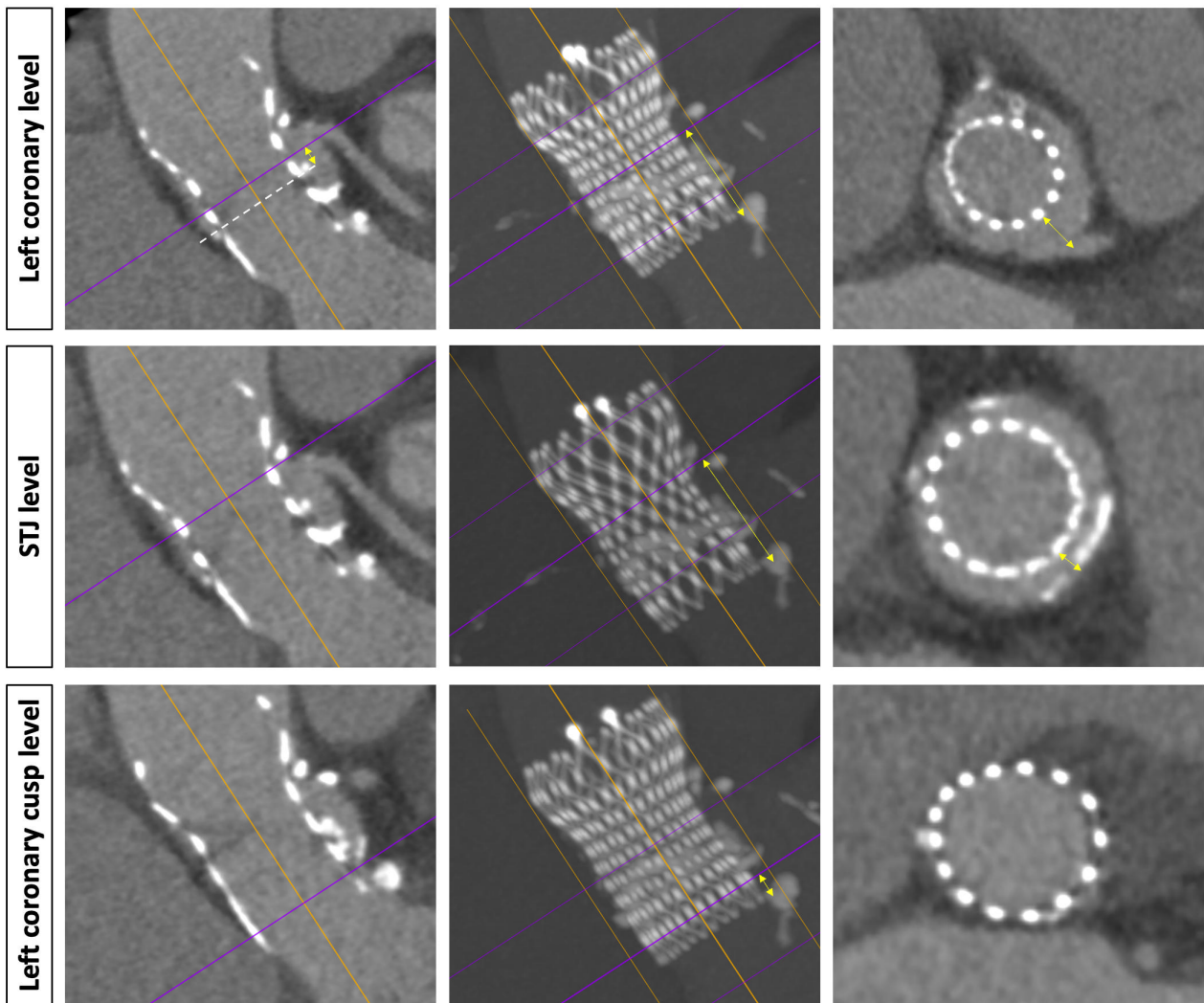


**Figure 9.** Computed tomography assessment after transcatheter aortic valve replacement. Left coronary level: bioprosthetic leaflets plane to coronary distance (left panel), coronary to valve inflow distance (central panel), valve to coronary distance (right panel). Sino-tubular junction (STJ) level: STJ to inflow distance (central panel), valve to STJ distance (right panel). Left coronary cusp level: implantation depth (central panel).

Coronary overlap and CA were measured according the ALIGN-TAVR Consortium recommendations (25). The double-oblique planes cutting through the THV centerline and both each coronary ostium midpoints, and those cutting through the THV centerline and

the sino-tubular junction (STJ) above the respective coronary ostium, were reconstructed (35). Then, the valve-to-coronary (VTC) distance and the valve-to-sinotubular junction (VTSTJ) distance were obtained by measuring horizontally from the coronary ostium midpoint, and the STJ directly above the coronary ostium, to the center of the blooming artifact of the metallic THV frame, respectively. The distance between THV leaflets plane and each coronary ostium was obtained by measuring perpendicularly from the nadir of the coronary ostium to that plane cutting the THV centerline lying above the THV inflow skirt.

### **Fluoroscopic and angiographic assessment post-TAVR**

Fluoroscopic evaluation of CA was also performed according to the ALIGN-TAVR Consortium recommendations (25). Examinations were performed by 2 readers (M.B. and G.C.).

### **Endpoints and definitions**

The primary endpoint was the rate of coronary ostia cannulation failure after TAVR. Secondary endpoints were the identification of factors associated with the inability to selectively cannulate coronary ostia after TAVR. Coronary cannulations were defined as “selective” when the catheter completely engaged the coronary ostium; “semi-selective” when the catheter was just in front of the coronary ostium without obtaining complete engagement, resulting in an adequate opacification of the coronary; or “unsuccessful” when it was deemed impossible to obtain selective or semi-selective coronary engagement, thus precluding proper opacification of the coronary artery with contrast media injection. CA was adjudicated according to the ALIGN-TAVR Consortium criteria (25). All clinical and echocardiographic outcomes were defined according to the Valve Academic Research Consortium-3 criteria (36).

## **Statistical analysis**

Continuous variables were reported as median and interquartile range (IQR). Categorical variables were reported as number and percentage. Comparisons between groups were performed using the U Mann-Whitney, the chi-square and the Fischer exact tests, as appropriate. Outcomes of the REACCESS-1 and the REACCESS-2 studies were compared by performing a pooled analysis including REACCESS-1 patients receiving only Evolut and ACURATE THV platforms. Univariable logistic regression analyses were performed to investigate factors associated with the inability to selectively cannulate coronary arteries after TAVR. Results were reported as odds ratio (OR) with a 95% confidence interval (CI). All statistical tests were performed two-tailed, and a significance level of  $p < 0.05$  was considered to indicate statistical significance. The statistical software SPSS 25.0 was used for all statistical analyses.

## **3.3 Results**

### **Baseline and procedural characteristics**

Baseline and procedural characteristics of patients according to the THV received, and to the feasibility of selective coronary ostia cannulation, are reported in **Tables 1-3**.

A total of 127 consecutive patients undergoing TAVR were enrolled. Patients had a median age of 83 years, and a median Society of Thoracic Surgeons (STS) mortality score of 3.3%. Eighty patients (63.0%) received the Evolut PRO/PRO+, whereas 47 (37.0%) the ACURATE Neo2 THV.

Patients receiving Evolut THVs had a higher oversizing degree (18.5% vs. 4.6%,  $p < 0.01$ ), but a lower rate of pre-dilatation (67.5% vs. 95.7%,  $p < 0.01$ ).

**Table 1.** Baseline and procedural characteristics of patients undergoing coronary artery angiography after transcatheter aortic valve replacement. Abbreviations: IQR, interquartile range; LVEF, left ventricular ejection fraction; STS, Society of Thoracic Surgeons.

	<b>Overall (n=127)</b>
Age, years, median [IQR]	83 [79;86]
Female, n (%)	75 (59.1)
Hypertension, n (%)	110 (86.6)
STS mortality score, %, median [IQR]	3.3 [2.1;5.6]
Diabetes, n (%)	48 (37.8)
Atrial fibrillation, n (%)	23 (18.1)
LVEF, %, median [IQR]	55 [54.5;60]
Evolut R, n (%)	22 (17.3)
Evolut PRO, n (%)	26 (20.5)
Evolut PRO+, n (%)	32 (25.2)
ACURATE Neo 2, n (%)	47 (37.0)
Oversizing, %, median [IQR]	15.5 [6.1;20.9]
Coronary artery disease, n (%)	36 (28.3)
Pre-dilatation, n (%)	99 (78.0)
Post-dilatation, n (%)	21 (16.7)
Angiographic misalignment, n (%)	
None/mild	99 (78.0)
Moderate	22 (17.3)
Severe	6 (4.7)

**Table 2.** Baseline and procedural characteristics of patients undergoing coronary artery angiography after transcatheter aortic valve replacement according to the type of valve used. Abbreviations: IQR, interquartile range; LVEF, left ventricular ejection fraction; STS, Society of Thoracic Surgeons.

	<b>Evolut (n=80)</b>	<b>ACURATE (n=47)</b>	<b>p-val</b>
Age, years, median [IQR]	83 [79;86]	83 [80;87]	0.581
Female, n (%)	53 (66.3)	22 (46.8)	0.040
Hypertension, n (%)	71 (88.8)	39 (83.0)	0.422
STS mortality score, %, median [IQR]	3.4 [2.0;5.6]	3.3 [2.2;5.7]	0.968
Diabetes, n (%)	29 (36.3)	19 (40.4)	0.706
Atrial fibrillation, n (%)	15 (18.8)	8 (17.0)	1.000
LVEF, %, median [IQR]	56 [55;60]	55 [50;60]	0.087
Evolut R, n (%)			
23 mm	3 (3.8)	-	
26 mm	11 (13.8)	-	
29 mm	8 (10.0)	-	
Evolut PRO, n (%)			
26 mm	12 (15.0)	-	
29 mm	14 (17.5)	-	
Evolut PRO+, n (%)			
23 mm	2 (2.5)	-	
26 mm	18 (22.5)	-	
29 mm	12 (15.0)	-	
34 mm	1 (1.3)	-	
ACURATE Neo 2, n (%)			
S	-	17 (36.2)	
M	-	17 (36.2)	
L	-	13 (27.6)	
Oversizing, %, median [IQR]	18.5 [16.2;22.3]	4.6 [2.0;6.8]	<0.001
Coronary artery disease, n (%)	23 (28.7)	16 (34.0)	0.255
Pre-dilatation, n (%)	54 (67.5)	45 (95.7)	<0.001
Post-dilatation, n (%)	15 (19.0)	6 (12.8)	0.462
Angiographic misalignment, n (%)			0.118
None/mild	67 (83.8)	32 (68.1)	
Moderate	10 (12.5)	12 (25.5)	
Severe	3 (3.8)	3 (6.4)	

**Table 3.** Baseline and procedural characteristics of patients undergoing coronary artery angiography after transcatheter aortic valve replacement according to the feasibility of selective re-engagement of coronary ostia. Abbreviations: IQR, interquartile range; LCA, left coronary artery; LVEF, left ventricular ejection fraction; RCA, right coronary artery; STS, Society of Thoracic Surgeons.

	<b>Unfeasible LCA or RCA cannulation (n=43)</b>	<b>Feasible LCA or RCA cannulation (n=84)</b>	<b>p-val</b>
Age, years, median [IQR]	83 [79;85]	83 [79.8;87]	0.520
Female, n (%)	29 (67.4)	46 (54.8)	0.187
Hypertension, n (%)	38 (88.4)	72 (85.7)	0.788
STS score, %, median [IQR]	3.51 [2.2;5.7]	3.29 [2.1;5.5]	0.643
Diabetes, n (%)	9 (20.9)	30 (46.4)	0.007
Atrial fibrillation, n (%)	8 (18.6)	15 (17.9)	1.000
LVEF, %, median [IQR]	55 [54.3;60]	55 [54;60]	0.930
Valve type, n (%)			
Evolut R	5 (11.6)	17 (20.2)	0.322
23 mm	0 (0.0)	3 (3.6)	-
26 mm	4 (9.3)	7 (8.3)	1.000
29 mm	1 (2.3)	7 (8.3)	0.264
Evolut PRO	12 (27.9)	14 (16.7)	0.165
23 mm	0 (0.0)	0 (0.0)	-
26 mm	5 (11.6)	7 (8.3)	0.538
29 mm	7 (16.3)	7 (8.3)	0.232
34 mm	0 (0.0)	0 (0.0)	-
Evolut PRO+	14 (32.5)	18 (21.4)	0.189
23 mm	1 (2.3)	1 (1.2)	1.000
26 mm	7 (16.3)	10 (11.9)	0.348
29 mm	6 (14.0)	6 (7.1)	0.220
34 mm	0 (0.0)	1 (1.2)	-
ACURATE Neo 2	12 (27.9)	30 (35.7)	0.429
S	4 (9.3)	9 (10.7)	1.000
M	5 (11.6)	12 (14.3)	0.788
L	3 (7.0)	9 (10.7)	0.750
Oversizing, %, median [IQR]	16.75 [8.7;21.5]	15.17 [5.7;20]	0.296
Coronary artery disease, n (%)	13 (30.2)	26 (30.9)	0.997
Pre-dilatation, n (%)	27 (62.8)	72 (85.7)	0.006
Post-dilatation, n (%)	11 (26.2)	10 (11.9)	0.073

## Coronary cannulation after TAVR

Outcomes of coronary cannulation according to THV received, and to the feasibility of selective coronary ostia cannulation, are reported in **Tables 4-6**.

**Table 4.** Characteristics of coronary artery angiography after transcatheter aortic valve replacement.  
Abbreviations: LCA, left coronary artery; RCA, right coronary artery

	<b>Overall (n=127)</b>
Unfeasible selective re-engagement of both coronaries, n (%)	5 (3.9)
Unfeasible selective re-engagement of LCA or RCA, n (%)	43 (33.9)
Unsuccessful cannulation of LCA or RCA, n (%)	7 (5.5)
<b>Left coronary artery</b>	
Selective LCA cannulation, n (%)	111 (87.4)
Semi-selective LCA cannulation, n (%)	13 (10.2)
Unsuccessful LCA cannulation, n (%)	3 (2.4)
Time for LCA cannulation, sec, median [IQR]	23 [3;80]
Dye contrast for LCA cannulation, ml, median [IQR]	2 [0;6]
<b>Right coronary artery</b>	
Selective RCA cannulation, n (%)	94 (74.0)
Semi-selective RCA cannulation, n (%)	27 (21.3)
Unsuccessful RCA cannulation, n (%)	5 (3.9)
Time for RCA cannulation, s, median [IQR]	50 [21.5;160]
Dye contrast for RCA cannulation, ml, median [IQR]	5.5 [2;13]

**Table 5.** Characteristics of coronary artery angiography after transcatheter aortic valve replacement according to the type of transcatheter heart valve used. Abbreviations: LCA, left coronary artery; RCA, right coronary artery

	<b>Evolut (n=80)</b>	<b>ACURATE (n=47)</b>	<b>p-val</b>
Unfeasible selective re-engagement of both coronaries, n (%)	5 (6.3)	0 (0.0)	-
Unfeasible selective re-engagement of LCA or RCA, n (%)	31 (38.8)	12 (25.5)	0.174
Unsuccessful cannulation of LCA or RCA, n (%)	6 (7.5)	1 (2.3)	0.258
<b>Left coronary artery</b>			
Selective LCA cannulation, n (%)	68 (85.0)	43 (91.5)	0.408
Semi-selective LCA cannulation, n (%)	10 (12.5)	3 (6.4)	0.369
Unsuccessful LCA cannulation, n (%)	2 (2.5)	1 (2.1)	1.000
Time for LCA cannulation, sec, median [IQR]	36 [5;120]	7 [0;30]	0.001
Dye contrast for LCA cannulation, ml, median [IQR]	4 [0;8]	0 [0;2]	<0.001
<b>Right coronary artery</b>			
Selective RCA cannulation, n (%)	55 (68.8)	39 (83.0)	0.095
Semi-selective RCA cannulation, n (%)	19 (23.8)	8 (17.0)	0.501
Unsuccessful RCA cannulation, n (%)	5 (6.3)	0 (0.0)	-
Time for RCA cannulation, s, median [IQR]	62.5 [31.3;186]	37.5 [14.8;93.8]	0.004
Dye contrast for RCA cannulation, ml, median [IQR]	8 [4;15]	2.5 [0;8.3]	<0.001

**Table 6.** Characteristics of coronary artery angiography after transcatheter aortic valve replacement according to the feasibility of selective re-engagement of coronary ostia. Abbreviations: LCA, left coronary artery; RCA, right coronary artery

	<b>Unfeasible selective re-engagement of LCA or RCA (n=43)</b>	<b>Feasible selective re-engagement of LCA and RCA (n=84)</b>	<b>p-val</b>
Angiographic misalignment, n (%)			0.276
None/mild	30 (69.8)	69 (82.1)	
Moderate	10 (23.3)	12 (14.3)	
Severe	3 (7.0)	3 (3.6)	
<b>Left coronary artery</b>			
Selective LCA angiography, n (%)	27 (62.8)	84 (100)	<0.001
Semi-selective LCA angiography, n (%)	13 (30.2)	0 (0.0)	-
Not opacized LCA, n (%)	3 (7.0)	0 (0.0)	-
Time for LCA cannulation, sec, median [IQR]	40 [2;165]	18 [3;60]	0.118
Dye contrast for LCA cannulation, ml, median [IQR]	4.5 [0;8.5]	0 [0;6]	0.007
<b>Right coronary artery</b>			
Selective RCA angiography, n (%)	11 (25.6)	84 (100.0)	<0.001
Semi-selective RCA angiography, n (%)	27 (62.8)	0 (0.0)	-
Not opacized RCA, n (%)	5 (11.6)	0 (0.0)	-
Time for RCA cannulation, s, median [IQR]	80 [40.8;285]	40 [20;120]	0.008
Dye contrast for RCA cannulation, ml, median [IQR]	8.5 [3.3;17.8]	4.5 [2;10]	0.012

Coronary ostia cannulation was unsuccessful in 7 patients (5.5%), and six of them received an Evolut THV (7.5% vs. 2.3%, p=0.26). In details, unfeasible cannulation of the LCA and RCA was reported in three (2.4%) and five patients (3.9%), respectively. Left coronary artery cannulation failure was similar between the two devices (2.5% vs. 2.1% for Evolut and ACURATE respectively, p=1.00) between the two THV types, whereas RCA cannulation failure was numerically higher in the Evolut group (6.3% vs. 0.0%, p=0.16). Overall, selective LCA and RCA cannulation was feasible in 87.4% and 74.0% of cases, respectively. The rate of selective coronary cannulation was numerically higher in the

ACURATE group (LCA: 85.0% vs. 91.5%,  $p=0.41$ ; RCA 68.8% vs. 83.0%,  $p=0.10$ ) (**Figure 10**).

Finally, unsuccessful coronary cannulation of both coronary arteries occurred only in Evolut recipients (6.3% vs. 0.0%,  $p=0.16$ ).

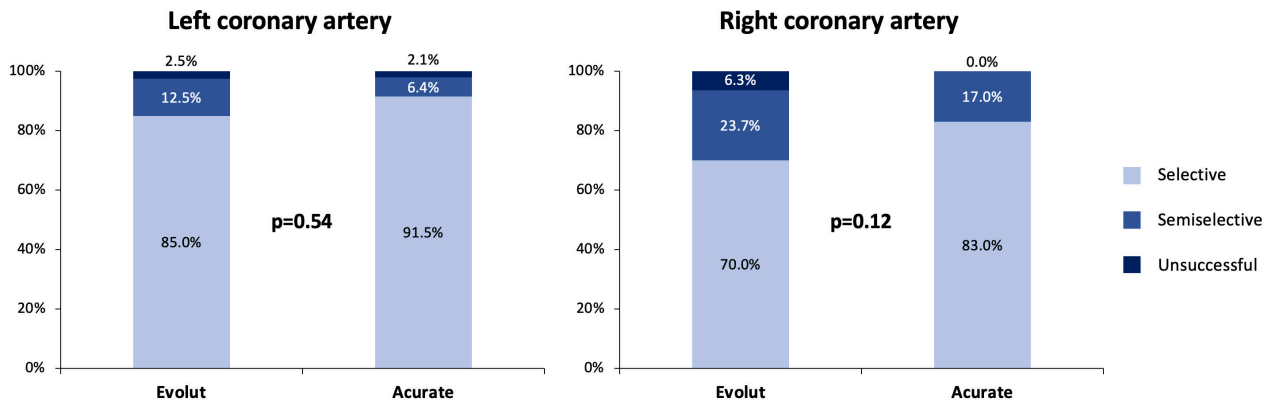


**Figure 10.** Coronary cannulation of right and left coronary arteries according to valve type.

### Post-TAVR CTA assessment

Post-TAVR CTA assessment was performed in 115 patients (90.6%) (**Supplementary Table 7**). Details of CTA assessment after TAVR, are reported in **Tables 8-10**.

**Table 7.** Characteristics and outcomes of patients undergoing or not computed tomography (CT) assessment after transcatheter aortic valve replacement (TAVR). Abbreviations: IQR, interquartile range; LCA, left coronary artery; LVEF, left ventricular ejection fraction; RCA, right coronary artery; STS, Society of Thoracic Surgeons.

	<b>No post-TAVR CT (n=12)</b>	<b>Post-TAVR CT (n=115)</b>	<b>p-val</b>
Female Sex, n (%)	7 (58.3)	50 (60.3)	0.710
Age, median years (IQR)	83 (80-87)	83 (79-86)	0.446
Diabetes, n (%)	4 (33.3)	32 (38.6)	0.645
Hypertension, n (%)	10 (83.3)	75 (90.4)	0.115
STS mortality score, median % (IQR)	3.7 (2.1-6.0)	3.2 (2.1-5.4)	0.468
LVEF, median % (IQR)	55 (50-58)	56.5 (55-60)	0.064
<b>Coronary cannulation after TAVR</b>			
Unsuccessful coronary cannulation	0 (0.0)	7 (6.1)	-
Selective LCA cannulation, n (%)	11 (91.7)	72 (86.7)	0.853
Semi-selective LCA cannulation, n (%)	1 (8.3)	8 (9.6)	0.934
Unfeasible LCA cannulation, n (%)	0 (0.0)	3 (3.6)	-
Selective RCA cannulation, n (%)	9 (75.0)	60 (72.3)	0.821
Semi-selective RCA cannulation, n (%)	3 (25.0)	17 (20.5)	0.672
Unfeasible RCA cannulation, n (%)	0 (0.0)	5 (6.0)	-

**Table 8.** Computed tomography angiography assessment after transcatheter aortic valve replacement according to the type of transcatheter heart valve used. Abbreviations: LCA, left coronary artery; LCC, left coronary cusp; NCC, non-coronary cusp; RCA, right coronary artery; RCC right coronary cusp; SoV, sinus of Valsalva; STJ, sino-tubular junction; VTSTJ, valve to sino-tubular junction

	<b>Overall (n=115)</b>
Moderate/severe misalignment, n (%)	23 (20.0)
Severe misalignment, n (%)	8 (7.0)
Commissural alignment, degrees, median [IQR]	16 [9;35]
Left coronary overlap, n (%)	12 (10.4)
Neo-commissure to LCA ostium, degree, median [IQR]	40 [26;48]
Inflow to LCA distance, mm, median [IQR]	25 [23;27.9]
Inflow to STJ distance at left SoV, mm, median [IQR]	6.5 [5;7.6]
Implant depth at LCC, mm, median [IQR]	5.3 [4.3;6.7]
Valve to LCA distance, mm, median [IQR]	1.4 [0.6;2.3]
VTSTJ at left SoV, mm, median [IQR]	5.2 [3.0;7.0]
Bioprosthetic valve plane to LCA distance, mm, median [IQR]	6.5 [5.0;9.0]
Right coronary overlap, n (%)	8 (7.0)
Neo-commissure to RCA ostium, degree, median [IQR]	42.5 [29.8;51.3]
Inflow to RCA distance, mm, median [IQR]	20 [18.3;22.6]
Inflow to STJ distance at right SoV, mm, median [IQR]	24 [22.8;27.1]
Implant depth at RCC, mm, median [IQR]	7.5 [5.6;9]
Valve to RCA, mm, median [IQR]	5 [3.8;6.0]
VTCSTJ at right SoV, mm, median [IQR]	1.2 [0;1.9]
Bioprosthetic valve plane to RCA distance, mm, median [IQR]	6.5 [5.0;9.0]
Implantation depth at NCC, mm, median [IQR]	5 [3.3;6.8]

**Table 9.** Computed tomography angiography assessment after transcatheter aortic valve replacement according to the type of transcatheter heart valve used. Abbreviations: LCA, left coronary artery; LCC, left coronary cusp; NCC, non-coronary cusp; RCA, right coronary artery; RCC right coronary cusp; SoV, sinus of Valsalva; STJ, sino-tubular junction; VTSTJ, valve to sino-tubular junction

	<b>Evolut (n=72)</b>	<b>ACURATE (n=43)</b>	<b>p-val</b>
Moderate/severe misalignment, n (%)	15 (20.8)	8 (19.0)	0.624
Severe misalignment, n (%)	6 (8.3)	2 (4.8)	0.468
Commissural alignment, degree, median [IQR]	18 [8;37]	14 [9;32.5]	0.423
Left coronary overlap, n (%)	8 (11.1)	4 (9.5)	0.755
Neocommissure to LCA ostium, degree, median [IQR]	39.5 [24;47.5]	42 [26;49.5]	0.618
Inflow to LCA distance, mm, median [IQR]	25.8 [23.8;28]	25 [21.2;27.5]	0.100
Inflow to STJ distance at left SoV, mm, median [IQR]	7.1 [5.8;8.57]	5.5 [4.45;6.6]	<0.001
Implant depth at LCC, mm, median [IQR]	5.35 [4.67;6.7]	4.8 [3.55;7.15]	0.163
VT to LCA distance, mm, median [IQR]	0.9 [0;1.6]	2.0 [1.4;2.7]	<0.001
VTSTJ at left SoV, mm, median [IQR]	6.6 [4;7.7]	3.5 [1.5;5.4]	<0.001
Bioprosthetic valve plane to LCA distance, mm, median [IQR]	6.85 [5;9.92]	6.3 [5.12;7.8]	0.256
Right coronary overlap, n (%)	5 (6.9)	3 (7.1)	1.000
Neo-commissure to RCA ostium, degree, median [IQR]	46.5 [32.8;52.5]	38.5 [25.5;46.5]	0.063
Inflow to RCA distance, mm, median [IQR]	19.9 [18;22.9]	20.5 [18.6;22.4]	0.574
Inflow to STJ distance at right SoV, mm, median [IQR]	24.2 [23.0;26.4]	23.7 [22.1;28.4]	0.992
Implant depth at RCC, mm, median [IQR]	8.1 [6.3;9.7]	6.6 [5.4;7.8]	0.003
VT to RCA, mm, median [IQR]	5.3 [4.1;6.1]	4.3 [3.1;5.7]	0.060
VTCSTJ at right SoV, mm, median [IQR]	0.9 [0.0;1.7]	1.4 [0.7;2.1]	0.132
Bioprosthetic valve plane to RCA distance, mm, median [IQR]	6.9 [5;9.9]	6.3 [5.1;7.8]	0.256
Implantation depth at NCC, mm, median [IQR]	5.8 [3.8;7.5]	4.2 [3.1;5.4]	0.010

**Table 10.** Computed tomography angiography assessment after transcatheter aortic valve replacement according to the feasibility of selective re-engagement of coronary ostia. Abbreviations: LCA, left coronary artery; LCC, left coronary cusp; NCC, non-coronary cusp; RCA, right coronary artery; RCC right coronary cusp; SoV, sinus of Valsalva; STJ, sino-tubular junction; VTSTJ, valve to sino-tubular junction

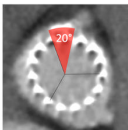
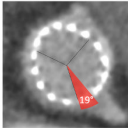
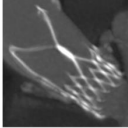
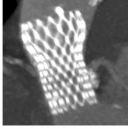
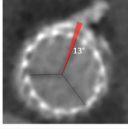
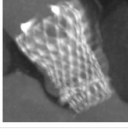

	<b>Unfeasible selective re-engagement of LCA or RCA (n=39)</b>	<b>Feasible selective re-engagement of LCA and RCA (n=76)</b>	<b>p-val</b>
Moderate/severe misalignment, n (%)	13 (33.3)	19 (25.0)	0.448
Severe misalignment, n (%)	4 (10.3)	7 (9.2)	1.000
Alignment concordance, n (%)	25 (64.1)	60 (78.9)	0.129
Alignment, degree, median [IQR]	20 [11;38]	14 [7;30.5]	0.088
<b>Left coronary cusp</b>			
CO with LCA, n (%)	5 (12.8)	11 (14.5)	1.000
Degree to LCA ostium, degree, median [IQR]	39 [25.5;47]	40 [25.5;50]	0.708
Inflow to LCA distance, mm, median [IQR]	19.5 [15.9;20.5]	18.5 [16.3;20.6]	0.772
Inflow to STJ distance at left SoV, mm, median [IQR]	25 [23;28]	25 [23.0;27.6]	0.556
Implant depth at LCC, mm, median [IQR]	7.1 [4.8;8.6]	6.2 [5.15;7.3]	0.263
VT to LCA distance, mm, median [IQR]	6.1 [4.7;7.5]	5 [3.8;6.2]	0.025
VTSTJ at left SoV, mm, median [IQR]	1.5 [0.7;2.3]	1.3 [0.5;2.3]	0.621
Bioprosthetic valve plane to LCA distance, mm, median [IQR]	5.6 [2.4;7.5]	5 [3;7]	0.504
<b>Right coronary cusp</b>			
CO with RCA, n (%)	6 (15.4)	4 (5.3)	0.135
Degree to RCA ostium, degree, median [IQR]	38.5 [29.8;53]	44 [28.3;50.8]	0.593
Inflow to RCA distance, mm, median [IQR]	20.5 [18.4;23.4]	19.8 [18;22.3]	0.325
Inflow to STJ distance at right SoV, mm, median [IQR]	25 [23.0;27.4]	23.7 [22.6;27.1]	0.423
Implant depth at RCC, mm, median [IQR]	7.85 [5.8;9.1]	7.4 [5.6;8.6]	0.405
VT to RCA, mm, median [IQR]	5.2 [3.8;6]	4.8 [3.6;6.0]	0.740
VTCSTJ at right SoV, mm, median [IQR]	1.25 [0.7;2.2]	1 [0;1.8]	0.311
Bioprosthetic valve plane to RCA distance, mm, median [IQR]	7 [5.3;10.1]	6.5 [5;8]	0.335
<b>Non-coronary cusp</b>			
Implantation depth at NCC, mm, median [IQR]	4.7 [3.3;6.9]	5.2 [3.6;6.8]	0.758

CA measured at post-TAVR CTA was similar among Evolut and ACURATE recipients (18° vs. 14°,  $p=0.42$ ). Implantation depth measured at non-coronary cusp was higher in ACURATE recipients (5.8 mm vs. 4.2 mm,  $p=0.01$ ).

Valve to LCA distance was greater in ACURATE recipients (0.9 mm vs. 2.0 mm,  $p<0.01$ ), whereas left VTSTJ distance was greater in Evolut recipients (6.6 mm vs. 3.5 mm,  $p<0.01$ ). Valve to RCA (5.3 mm vs. 4.3 mm,  $p=0.06$ ) and right VTSTJ (0.9 mm vs. 1.4 mm,  $p=0.13$ ) distances were similar between Evolut and ACURATE recipients.

The rates of right (6.9% vs. 7.1%,  $p=1.0$ ) and left (11.1% vs. 9.5%,  $p=0.76$ ) coronary overlap with the THV commissure were similar between Evolut and ACURATE recipients.

Details of patients with unsuccessful coronary cannulation after TAVR were reported in **Figure 11**.

		Coronary impairment	THV	Coronary eccentricity	Coronary overlap	Commissure misalignment	Mean SoV diameter	Mean STJ diameter	Coronary height	THV oversizing	VTC	VTSTJ	Valve plane to coronary distance	Implant depth at NCC
Patient #1		RCA cannulation impaired due to commissure proximity	PRO 29mm	Severe	No	Mild	29 mm	28 mm	16 mm	17.5%	2.5 mm	0.5 mm	11.5 mm	6.9 mm
Patient #2		LCA cannulation impaired due to commissure proximity	PRO 26mm	None	No	Severe	28 mm	26 mm	13 mm	20.8%	5.4 mm	0.9 mm	5.5 mm	5.2 mm
Patient #3		LCA cannulation impaired due STJ sealing by THV's upper crown	Neo2 size M	Mild	No	None	29.5 mm	30 mm	14 mm	7.2%	7.3 mm	1.4 mm	-1.5 mm	1.0 mm
Patient #4		Coronary cannulation impaired due to native leaflets encumbrance	PRO+ 26mm	None	No	None	29 mm	25.5 mm	13 mm (LCA) 15 mm (RCA)	10.3%	4.7 mm (LCA) 3.8 mm (RCA)	1.1 mm (LCA) 1.1 mm (RCA)	5.0 mm for both LCA and RCA	2.5 mm
Patient #5		RCA cannulation impaired due to commissure overlap	PRO+ 26mm	None	Yes	Severe	29 mm	26.5 mm	11 mm	12.7%	3.6 mm	2.2 mm	3.5 mm	4.5 mm
Patient #6		RCA cannulation impaired due to proximity with STJ	PRO 26mm	Mild	No	None	31 mm	30 mm	17 mm	11.8%	4.4 mm	0 mm	8 mm	5.9 mm
Patient #7		RCA cannulation impaired due to proximity with calcific STJ	PRO 26mm	Severe	No	Mild	30 mm	29 mm	16 mm	14.5%	1.8 mm	0.9 mm	5 mm	3.5 mm

**Figure 11.** Characteristics of patients with unfeasible coronary cannulation following transcatheter aortic valve replacement. LCA, left coronary artery; NCC, non-coronary cusp; RCA, right coronary artery; SoV, sinus of Valsalva; STJ, sino-tubular junction; THV, transcatheter heart valve; VTC, valve to coronary; VTSTJ, valve to STJ.

## Predictors of unsuccessful selective coronary cannulation

Univariable logistic regression analyses for unsuccessful selective LCA, RCA or both coronary arteries were reported in **Tables 11-13**.

Univariable logistic regression analyses for unsuccessful selective LCA and RCA considering separately Evolut and ACURATE recipients, were reported in **Tables 14-15**.

**Table 11.** Univariable logistic regression analysis of computed tomography angiography characteristics associated with failure of selective left coronary cannulation after transcatheter aortic valve replacement. Abbreviations: LCA, left coronary artery; LCC, left coronary cusp; SoV, sinus of Valsalva; STJ, sino-tubular junction; VTSTJ, valve to sino-tubular junction

	<b>Odds ratio (95% confidence interval)</b>	<b>p-val</b>
Left coronary ostium overlap	0.55 (0.06-4.78)	0.592
Severe misalignment	2.44 (0.43-14.00)	0.315
Inflow to STJ distance at left SoV	0.91 (0.75-1.11)	0.354
Implant depth at LCC	0.93 (0.69-1.24)	0.603
Valve to LCA distance	1.15 (0.83-1.60)	0.397
VTSTJ at left SoV	0.75 (0.42-1.32)	0.317
Bioprosthetic valve plane to LCA distance	0.91 (0.76-1.10)	0.324
ACURATE valve	0.53 (0.16-1.74)	0.293

**Table 12.** Univariable logistic regression analysis of computed tomography angiography characteristics associated with failure of selective right coronary cannulation after transcatheter aortic valve replacement. Abbreviations: RCA, right coronary artery; RCC right coronary cusp; SoV, sinus of Valsalva; STJ, sino-tubular junction; VTSTJ, valve to sino-tubular junction

	<b>Odds ratio (95% confidence interval)</b>	<b>p-val</b>
Right coronary ostium overlap	5.59 (1.21-25.82)	0.028
Severe misalignment	1.77 (0.39-8.11)	0.463
Inflow to STJ distance at right SoV	1.03 (0.90-1.18)	0.653
Implant depth at RCC	1.13 (0.92-1.39)	0.253
Valve to RCA distance	0.98 (0.75-1.29)	0.891
VTCSTJ at right SoV	1.23 (0.77-1.95)	0.385
Bioprosthetic valve plane to RCA distance	1.08 (0.93-1.25)	0.318
ACURATE valve	0.48 (0.20-1.18)	0.110

**Table 13.** Univariable logistic regression analysis of computed tomography angiography characteristics associated with failure of selective coronary cannulation of both coronary arteries after transcatheter aortic valve replacement. Abbreviations: NCC, non-coronary cusp.

	<b>Odds ratio (95% confidence interval)</b>	<b>p-val</b>
Severe misalignment	24.67 (1.94-312.93)	0.013
Implantation depth at NCC	0.81 (0.47-1.38)	0.431

**Table 14.** Univariable logistic regression analysis of computed tomography angiography characteristics associated with failure of selective left coronary cannulation after transcatheter aortic valve replacement, considering two separate cohort of patients according to the valve type. Abbreviations: LCA, left coronary artery; LCC, left coronary cusp; SoV, sinus of Valsalva; STJ, sino-tubular junction; VTSTJ, valve to sino-tubular junction

	Evolut cohort		ACURATE cohort	
	Univariable	p-val	Univariable	p-val
Left coronary ostium overlap	0.86 (0.09-8.27)	0.857	-	
Severe misalignment	3.90 (0.56-20.03)	0.168	-	
Inflow to STJ distance at left SoV	0.86 (0.66-1.13)	0.289	0.95 (0.79-1.30)	0.769
Implant depth at LCC	0.95 (0.67-1.34)	0.767	0.76 (0.38-1.53)	0.441
Valve to LCA distance	0.94 (0.57-1.54)	0.799	1.41 (0.86-2.30)	0.178
VTSTJ at left SoV	0.60 (0.22-1.59)	0.302	0.88 (0.38-2.09)	0.775
Bioprosthetic valve plane to LCA distance	0.82 (0.61-1.11)	0.201	0.94 (0.68-1.28)	0.693

**Table 15.** Univariable logistic regression analysis of computed tomography angiography characteristics associated with failure of selective left coronary cannulation after transcatheter aortic valve replacement, considering two separate cohort of patients according to valve type. Abbreviations: RCA, right coronary artery; RCC right coronary cusp; SoV, sinus of Valsalva; STJ, sino-tubular junction; VTSTJ, valve to sino-tubular junction

	Evolut cohort		ACURATE cohort	
	Univariable	p-val	Univariable	p-val
Right coronary ostium overlap	9.85 (1.00-96.66)	0.050	3.12 (0.23-43.02)	0.394
Severe misalignment	2.14 (0.38-11.98)	0.386	-	
Inflow to STJ distance at right SoV	1.02 (0.87-1.21)	0.774	1.06 (0.82-1.38)	0.638
Implant depth at RCC	1.07 (0.85-1.35)	0.551	1.03 (0.57-1.85)	0.925
Valve to RCA distance	0.98 (0.68-1.42)	0.917	0.82 (0.50-1.34)	0.426
VTCSTJ at right SoV	1.49 (0.86-2.57)	0.157	0.90 (0.32-2.51)	0.840
Bioprosthetic valve plane to RCA distance	1.05 (0.89-1.25)	0.554	1.10 (0.80-1.50)	0.559

No anatomical factors associated with the inability to selective cannulate the LCA, were detected.

Coronary ostia overlap with the THV commissure was the only factor associated with the inability to selectively cannulate the RCA (OR 5.6, 95% CI 1.2-25.8,  $p=0.03$ ). Of note, this finding was not confirmed when analyzing the ACURATE cohort separately ( $p=0.38$ ).

Severe misalignment the only factor associated with the inability to selectively cannulate both coronary artery (OR 24.7, 95% CI 1.9-312.9,  $p=0.01$ ), with events occurring only in patients receiving Evolut THV.

### **3.4 Discussion**

The necessity to ensure an easy coronary re-access after TAVR has recently gained particular importance due to the expanding indications to younger patients. Indeed, it has been demonstrated that patients undergoing acute coronary syndromes after TAVR have worse outcomes compared to patients without prior TAVR, and this was mainly related to the difficulties of obtaining a proper coronary cannulation due to the presence of the THV frame (32,33). The introduction of a patient-specific CA technique in TAVR practice promised to improve patients' outcomes by lowering the possibility to have a bioprosthetic commissure overlapping the coronary ostia (26).

The REACCESS-2 study was the first, prospective study aiming at investigating coronary re-access after TAVR in the current practice using self-expanding, supra-annular bioprosthesis with the routine application of CA technique for THV deployment, and at assessing potential anatomical and prosthesis-related characteristics associated with coronary cannulation impairment by using post-procedural CTA assessment.

The main findings were:

1. Unsuccessful coronary artery cannulation was reported in 5.5% of patients, with 6 out of 7 cases occurring in patients receiving the Evolut THV. Selective coronary re-

- engagement was obtained in 87.4% and 74.0% of cases for LCA and RCA, respectively, with rates being numerically higher in ACURATE recipients.
2. CA was obtained in most of cases, with no difference between Evolut and ACURATE devices. Severe THV misalignment impaired coronary reaccess after TAVR only in Evolut recipients, especially when a bioprosthetic commissure overlapped the right coronary ostium.
  3. No spatial relationship between THV and surrounding aortic root anatomy was associated with the impossibility to obtain a selective coronary cannulation after TAVR.

It is interesting to put these findings into perspectives with those reported in the REACCESS-1 study. This was the first investigating the feasibility of coronary reaccess after TAVR in consecutive patients receiving both self-expanding and balloon-expandable THVs. Overall, the rate of unsuccessful coronary re-access was 7.7%, whereas this rate was remarkably higher among patients receiving the Evolut device (22/123, 17.9%) (5). Of note, alignment of THV commissures was random in the RE-ACCESS 1 study.

In the REACCESS-2 study, unfeasibility of coronary re-access after TAVR with Evolut THV platform using CA technique markedly reduced from 17.9% to 7.5% (**Figures 12-13**).

Nevertheless, patients receiving Evolut THV confirmed a numerically higher rate of unsuccessful coronary re-access compared to patients receiving the ACURATE THV (7.5% vs. 2.3%,  $p=0.26$ ).

## Coronary cannulation following TAVR using self-expanding devices with or without patient-specific commissural alignment

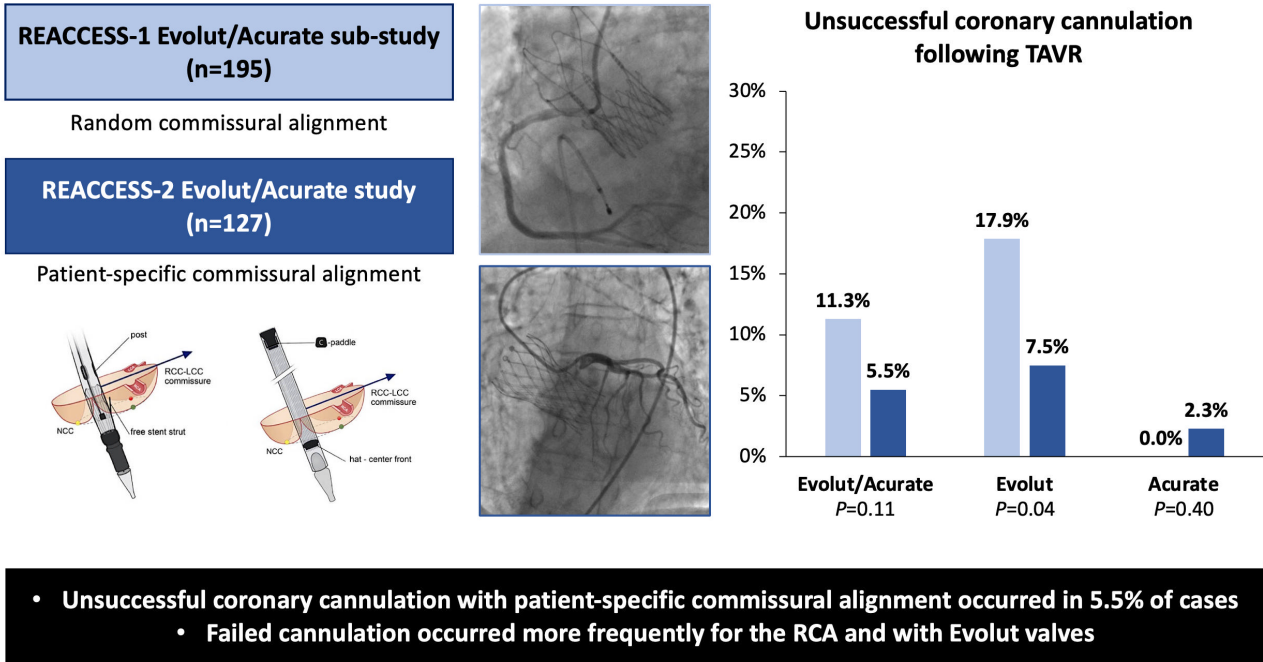


**Figure 12.** Coronary access following transcatheter aortic valve replacement (TAVR). Unsuccessful coronary cannulation after TAVR with (REACCESS-2) and without (REACCESS-1) patient-specific commissural alignment using the ACURATE and the Evolut valve platforms.

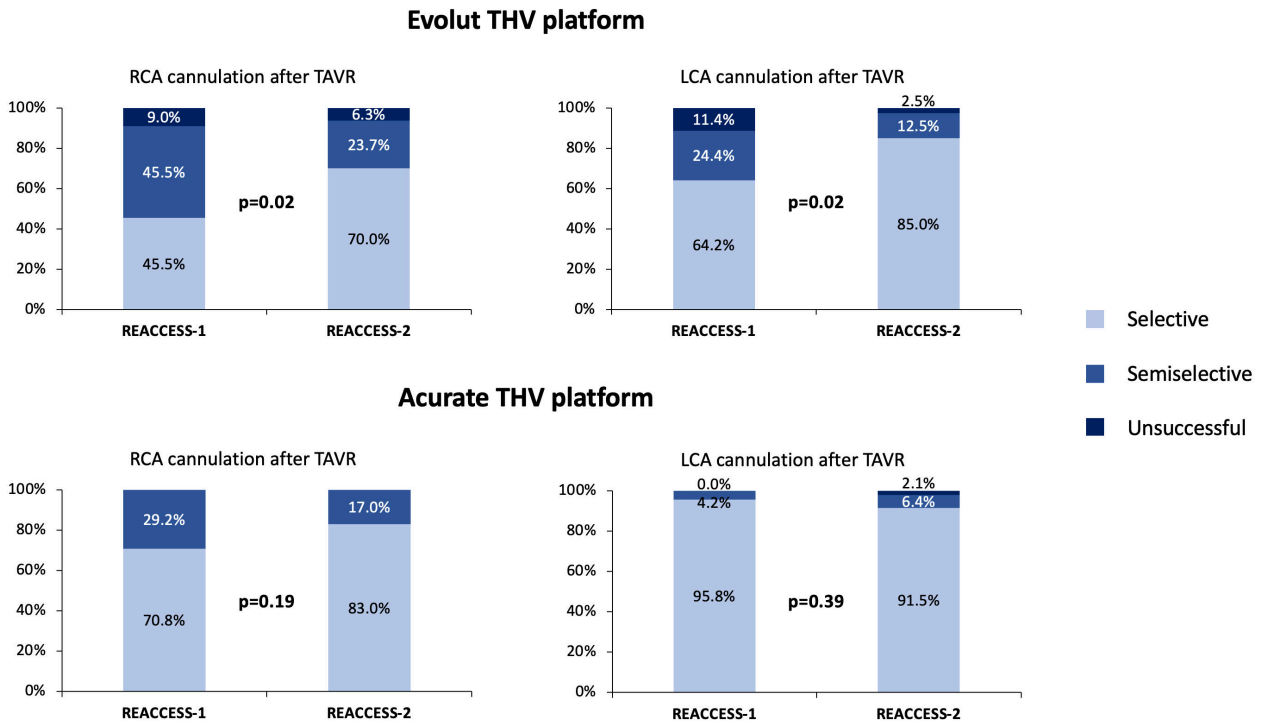


**Figure 13.** Coronary cannulation following transcatheter aortic valve replacement with (REACCESS 2) and without (REACCESS 1) commissural alignment using the ACURATE and the Evolut valve platforms.

Besides, rates of selective LCA (85.0% vs. 91.5%,  $p=0.41$ ) and RCA (68.8% vs. 83.0%,  $p=0.10$ ) cannulation after TAVR were numerically higher in ACURATE THV recipients.

To date, the ALIGN-ACCESS was the sole study that investigated the impact of alignable THVs on coronary re-access after TAVR. It reported that unsuccessful coronary cannulation was more frequent in patients receiving mis-aligned, supra-annular Evolut or ACURATE THV platforms (11% vs. 3%), and that commissural misalignment was an independent predictor of selective coronary cannulation impairment (11).

The REACCESS-2 study included a routine post-procedural CTA assessment of THV position and orientation. Adopting the CA implantation technique, severe THV misalignment was avoided in up to 93% of cases, with no difference between Evolut and ACURATE devices. We reported that severe commissural misalignment impaired coronary re-access only in Evolut recipients. In this group, right coronary overlap was associated with the inability to selective engage the RCA.

These findings highlight the greater impact of the THV design on coronary re-access after TAVR compared to the importance of CA. Indeed, the open-cell design of the ACURATE platform, seems to ensure an easier coronary cannulation after TAVR even in those cases in whom CA was not obtained. However, it must be underlined that CA still maintains a crucial role for all THVs when considering the possibility to perform a leaflet laceration in case of re-do TAVR.

The cannulation of RCA implies greater catheter maneuvers per se compared to LCA cannulation. The close-cell design of the Evolut THV platform, particularly impairs re-engagement of the RCA, being catheter maneuvers more restricted by the THV frame itself. Moreover, despite in the study optimal working views for coronary cannulation after TAVR were systematically adopted by perpendicularly aligning the THV frame and the intended coronary ostium, the impossibility to obtain extreme fluoroscopic angulations could have had an impact on RCA engagement after TAVR.

Of note, the sole ACURATE patient with unsuccessful LCA cannulation, had the coronary originating below the bioprosthetic leaflets plane at post-TAVR CTA assessment, with upper crown extending above the STJ (**Figure 14**).

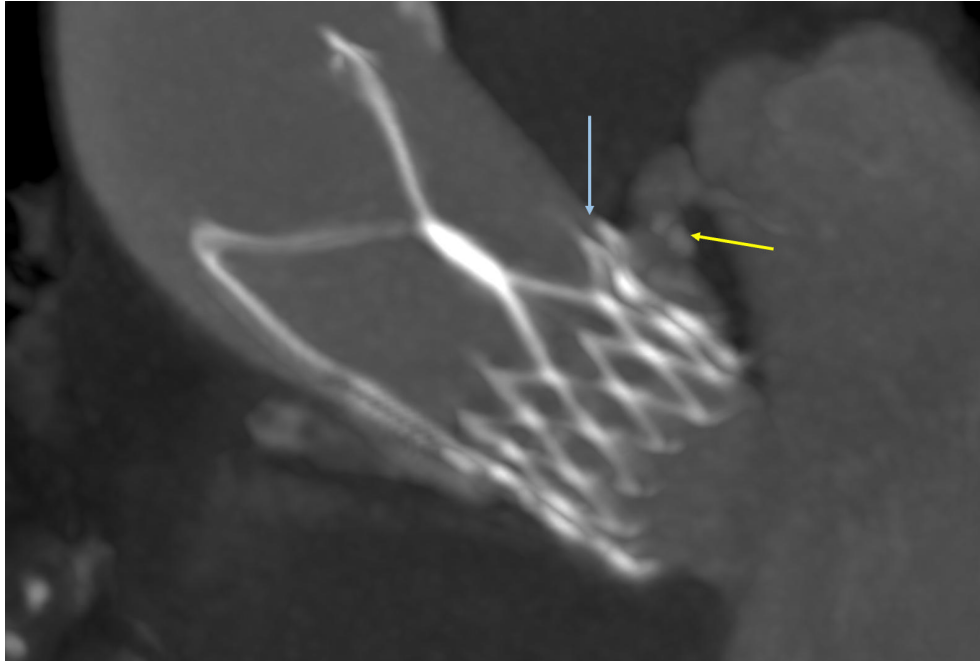


**Figure 14.** Volume-rendering reconstruction of computed tomography acquisitions performed in the patient with unsuccessful left coronary cannulation after transcatheter aortic valve replacement using the ACURATE Neo 2 valve. The left coronary artery lies below the bioprosthetic leaflets plane (yellow arrow) whereas the ACURATE upper crown extends above the sino-tubular junction (blue arrow).

Finally, implantation height, VTC and VTSTJ measured at post-TAVR CTA assessment were not associated with coronary re-access impairment after TAVR. These findings might have been impacted by the results emerged from the REACCESS-1 study. As its consequence, in this study TAVR devices were used to be selected according to patients' aortic root anatomy, and implantation depth was used to be adapted according to the risk of permanent pacemaker implantation and the expected risk of coronary re-access impairment.

In conclusion, compared to the previous study, coronary re-access improved after TAVR in contemporary practice using self-expanding, supra-annular THVs implanted aiming at CA. Nevertheless, a large-cell THV design seems to be the most impactful factor for an easier coronary re-access after TAVR. Albeit the already available Evolut FX (Medtronic Inc)

iteration has improved characteristics that promise to achieve a better commissural alignment with the current technique, a revised cell design is awaited to definitely tackle the issue of coronary re-access after TAVR with this THV platform. Besides, modified delivery system enabling the intra-annular rotation of TAVR devices during deployment, are necessary to optimize CA.

### **3.5 Limitations**

The relatively small sample size of the study significantly affected the results and therefore they should be considered only hypothesis-generating. In particular, the few absolute events of study endpoints might have decreased the statistical power of the study. Larger studies are required to confirm these findings.

Besides, due to the non-randomized nature of the study, the operators' choice of the THV type and implantation depth might have affected the results of the study. The increased experience of operators in performing coronary cannulation after TAVR might have played a determinant role in study outcomes. Finally, stiffness and tortuosity of aorto-femoral axes might have affected outcomes of CA attempts.

## **4. TRANSCATHETER HEART VALVE FRAME DINAMICITY ACROSS THE CARDIAC CYCLE AFTER TAVR WITH COMMISSURAL ALIGNMENT**

### **4.1 Introduction**

Transcatheter aortic valve replacement (TAVR) has progressively redefined the treatment of severe aortic stenosis (AS), initially reserved for patients deemed inoperable or at high surgical risk, and now established as a cornerstone therapy across the full spectrum of risk categories (1,2).

Advancements in device technology, procedural techniques, and operator experience have led to significant improvements in short- and mid-term results (37–43).

Despite these encouraging findings, long-term durability of TAVR platforms remains an open question, particularly as their use expands to younger, lower-risk patients with longer life expectancy. Several procedural and anatomical factors — including valve crimping, asymmetric frame expansion, and interaction with calcified native anatomy— raise concerns regarding leaflet motion and structural integrity over time (44,45).

More recently, the biomechanical behaviour of transcatheter heart valves (THVs) has emerged as a complementary area of investigation, alongside these established mechanical issues. Most available data derive from in vitro studies and computational models, which have provided valuable insights into how valve design, frame expansion, and flow dynamics may contribute to leaflet thrombosis and SVD (46–49) . However, clinical in vivo data remain sparse; in particular, the dynamic interaction between THV frames and the native aortic root throughout the cardiac cycle has not been adequately explored. This is particularly relevant for self-expanding (SE) valves, whose nitinol frames allow dynamic, cyclical expansion.

In this context, our study aimed at assessing the in-vivo behaviour of SE THV frames during the cardiac cycle, by analysing 4-dimensional computed tomography angiography (4D-CTA) acquisitions performed after TAVR, focusing on the interaction of the bioprosthetic stents with the aortic root at multiple levels, and on its potential role in determining subclinical valve deterioration.

## **4.2 Methods**

### **Study design and population**

This was a pre-specified analysis of the prospective, single-center, observational REACCES-2 study (Reobtain Coronary Ostia Cannulation Beyond Transcatheter Aortic Valve Stent 2). Study details have been previously published (50).

For the purpose of this analysis, we included only patients who received a SE device — specifically Evolut R/PRO/PRO+ (Medtronic), or ACURATE Neo2 (Boston Scientific) — with available pre- and post-TAVR ECG-gated computed tomography angiography (CTA) of sufficient quality to allow for detailed stent frame assessment (**Figure 15**). Exclusion criteria were consistent with the original study and included: prior aortic bioprosthesis degeneration, known coronary ostial chronic total occlusion, native bicuspid aortic valve, device failure, hemodynamic instability during the procedure, and stage IV or V chronic kidney disease.

The study was conducted in accordance with the principles of the Declaration of Helsinki, and the protocol was approved by the local institutional review board. The authors wrote all drafts of the paper and vouch for the integrity of and completeness of the data and analyses.

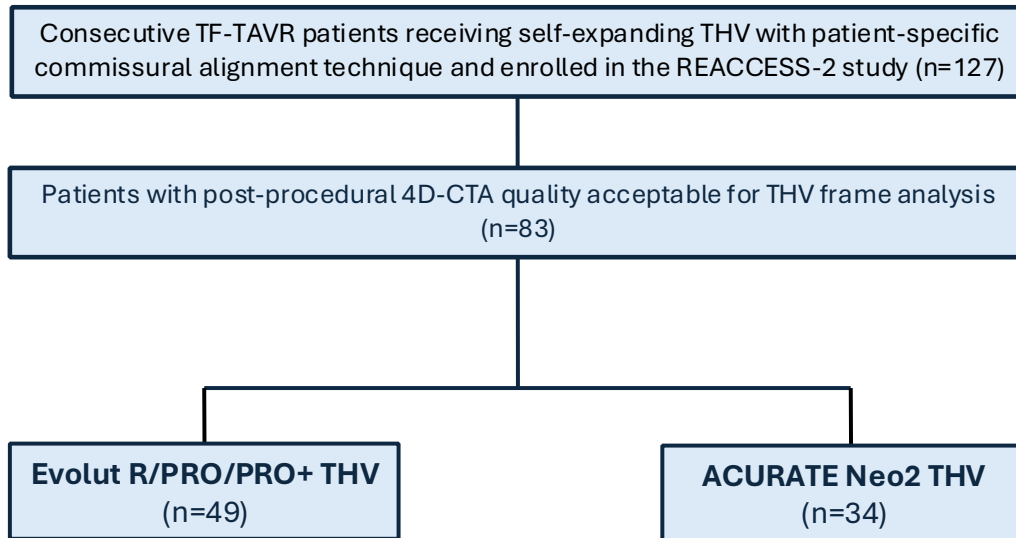


**Figure 15.** Study participant flow

### **Post-TAVR CTA assessment**

Post-TAVR, ECG-gated CTA datasets were anonymized and independently reviewed by three experienced cardiac computed tomography readers (G.C., M.B., V.G.) following a standardized imaging protocol. Key measurements are illustrated in **Figure 16**.

For each patient, THV frame measurements were performed at three predefined levels, perpendicularly to the THV long axis: the inflow (corresponding to the cross-sectional plane passing through the bottom of the frame), the virtual basal ring (VBR, defined as the cross-sectional plane passing through the nadir of the native non-coronary cusp), and the bioprosthetic leaflet plane (BLP, defined as the cross-sectional plane passing through the nadir of the prosthetic valve leaflets) (17,18). Working planes were obtained using multiplanar reconstruction (MPR) in systolic and diastolic phases acquisitions. Maximum and minimum diameters, and the planimetric perimeter were measured at each pre-specified level. Stent expansion was assessed by calculating the absolute variation between systolic and diastolic measurements at each level.

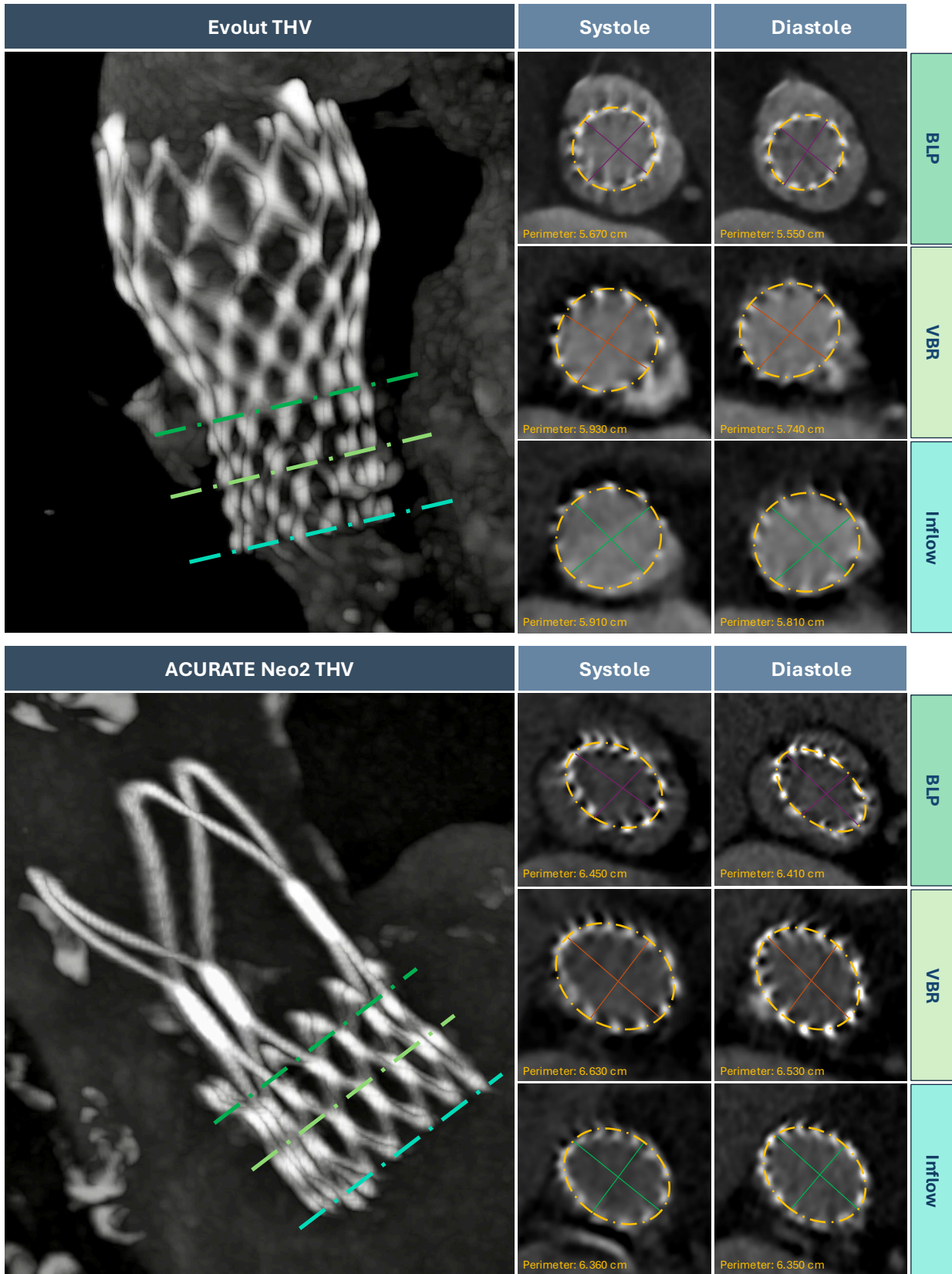


**Figure 16.** Four-dimensional computed tomography angiography assessment of self-expanding transcatheter heart valves (THVs) frame at multiple levels in systolic and diastolic phases. BLP: bioprosthesis leaflets plane; VBR: virtual basal ring

Hypo-attenuated leaflets thickening (HALT) was defined as focal thickening with reduced attenuation involving at least one leaflet, visible in both systolic and diastolic phases (19,20). HALT was typically identified on short-axis or long-axis reconstructions, according to Valve Academic Research Consortium (VARC) 3 criteria (24). Restricted leaflet motion (RLM) was defined as a reduction in the systolic excursion of at least one leaflet, best assessed on long-axis views during systole. Leaflets were classified as normal, mildly, or severely reduced motion, according to previously published criteria (19,21). All measurements were performed on ECG-gated CTA datasets reconstructed with a slice thickness of 0.5 mm.

### **Study Endpoints**

The primary endpoint was to assess stent expansion of SE THVs across the cardiac cycle at post-TAVR 4-D CTA, and potential differences between THV platforms.

The secondary endpoint was to detect the presence of HALT and/or RLM, and its association with stent expansion.

### **Statistical analysis**

Continuous variables were reported as median and interquartile range (IQR). Categorical variables were reported as number and percentage. Comparisons between groups were performed using the U Mann-Whitney, the chi-square and the Fischer exact tests, as appropriate. Univariable and multivariable logistic regression analyses were performed to investigate factors associated with THV frame expansion. A stepwise model was used, retaining variables with  $p < 0.10$ . Results were reported as odds ratio (OR) with a 95% confidence interval (CI). All statistical tests were performed two-tailed, and a significance level of  $p < 0.05$  was considered to indicate statistical significance. The statistical software SPSS 25.0 was used for all statistical analyses.

## 4.3 Results

### Baseline and Procedural Characteristics

Baseline and procedural characteristics are reported in **Tables 16-18**.

A total of 83 patients underwent TAVR with self-expanding valves: 49 received Evolut (n=10 Evolut R, n=20 Evolut PRO, and n=19 Evolut PRO+) and 34 ACURATE Neo2 (**Figure 15**). Median age was 83 years [79–86], 59% were female, and median Society of Thoracic Surgeons (STS) risk score was 3.2% [2–4.5]. Baseline clinical and echocardiographic characteristics were similar between Evolut and ACURATE recipients (**Table 16**).

**Table 16.** Baseline characteristics of the study population Data are presented as median [IQR] or n (%). AVA: aortic valve area; BMI: Body Mass Index; CAD: coronary artery disease; eGFR: estimated Glomerular Filtration Rate; LVEF: left ventricular ejection fraction; STS: Society of Thoracic Surgeons.

	<b>Overall (n = 83)</b>	<b>Evolut (n = 49)</b>	<b>ACURATE (n = 34)</b>	<b>p-val</b>
Age, years	83 [79-86]	83 [79-85]	82.5 [79-86.5]	0.366
Female sex	49 (59.0)	32 (65.3)	17 (50.0)	0.181
BMI	25 [23-28]	25 [23-29]	25 [24-28]	0.487
eGFR, mL/min/1.73m <sup>2</sup>	54.5 [41.2-70.6]	55 [40.2-69.7]	51.6 [42.5-75]	0.204
Hypertension	75 (90.4)	46 (93.9)	29 (85.3)	0.263
Diabetes mellitus	31 (37.3)	16 (32.7)	15 (44.1)	0.358
Atrial fibrillation	13 (15.7)	9 (18.4)	4 (11.8)	0.544
CAD	28 (33.7)	17 (34.7)	11 (32.4)	1.000
STS mortality score, (%)	3.2 [2-4.5]	3.2 [2.1-4.5]	3.2 [2-5.5]	0.704
<b>Echocardiographic assessment</b>				
LVEF, (%)	56 [55-60]	55.5 [54.8-60]	57.5 [55-60]	0.322
Mean Gradient (mmHg)	50 [44-60]	50 [44.8-60]	49.5 [44-59.5]	0.934
AVA (cm <sup>2</sup> )	0.7 [0.6-0.8]	0.6 [0.6-0.8]	0.7 [0.6-0.7]	0.964

At pre-procedural CTA assessment, leaflet calcium was more commonly severe (73.5%) whereas calcium at left ventricular outflow tract (LVOT) absent or mild (95.2%). No differences in both leaflets ( $p=0.681$ ) or LVOT ( $p=0.560$ ) between Evolut and ACURATE groups were reported (**Table 17**).

**Table 17.** Native aortic valve calcium assessment by pre-procedural computed tomography angiography. Data are presented as n (%). Abbreviations: LVOT = left ventricular outflow tract.

	<b>Overall (n=83)</b>	<b>Evolut (n=49)</b>	<b>ACURATE (n=34)</b>	<b>p-val</b>
<b>Leaflets calcifications, n (%)</b>				<b>0.681</b>
Mild	6 (7.2)	4 (8.2)	2 (5.9)	
Moderate	15 (18.1)	10 (20.4)	5 (14.7)	
Severe	61 (73.5)	34 (69.4)	27 (79.4)	
<b>LVOT calcifications, n (%)</b>				<b>0.560</b>
None/mild	79 (95.2)	45 (91.8)	34 (100)	
Moderate	2 (2.4)	2 (4.1)	0 (0.0)	
Severe	1 (1.2)	1 (2.0)	0 (0.0)	

Pre-dilatation was performed more frequently with ACURATE Neo2 (94.1% vs. 71.4%;  $p = 0.022$ ), whereas post-dilatation rates were similar (11.8% vs. 12.2% for ACURATE and Evolut, respectively;  $p = 1.00$ ). Predicted oversizing was higher for Evolut THV (15.0% vs. 13.5%;  $p = 0.003$ ). At final fluoroscopy, commissural alignment was good and comparable between the two platforms ( $p=0.64$ ), with low rates of severe misalignment (8.8% vs. 6.1% for ACURATE and Evolut, respectively) (**Table 18**).

**Table 18.** Procedural characteristics. Data are presented as median [IQR] or n (%).

	<b>Overall (n = 83)</b>	<b>Evolut (n = 49)</b>	<b>ACURATE (n = 34)</b>	<b>p-val</b>
<b>Valve size</b>				-
23 mm	18	3	15	
25 mm	-	-	10	
26 mm	-	24	-	
27 mm	-	-	9	
29 mm	-	22	-	
Pre-dilatation, n (%)	67 (80.7)	35 (71.4)	32 (94.1)	0.022
Post-dilatation, n (%)	10 (12.0)	6 (12.2)	4 (11.8)	1.00
Oversizing, (%)	14.2 [8.7-19.8]	15 [9.6-20.4]	13.5 [7.9-18.8]	0.003
<b>Angiographic misalignment, n (%)</b>				0.640
None/mild	64 (77.1)	40 (81.6)	24 (70.6)	
Moderate	14 (16.9)	7 (14.3)	7 (20.6)	
Severe	6 (7.2)	3 (6.1)	3 (8.8)	

#### 4-D CTA THV stent assessment

The THV frame assessment at the three levels of interest were reported in **Table 19**. The median interval from TAVR to post-procedural 4-D CTA was 35 days.

**a) BLP:** THV minimum and maximum diameters, and perimeter were 19.3 mm, 23.5 mm and 67.3 mm in systole, respectively, and 19.6 mm, 23.4 mm and 67.5 mm in diastole, respectively. The minimum diameter was significantly larger in Evolut THV both in systole (median 19.8 mm vs. 18.2 mm,  $p = 0.012$ ) and in diastole (median 19.9 mm vs. 18.2 mm,  $p = 0.008$ ). No significant differences were observed between the two platforms in terms of maximum diameter (systole,  $p = 0.650$ ; diastole,  $p = 0.915$ ) and perimeter (systole,  $p = 0.441$ ; diastole,  $p = 0.234$ ).

**b) VBR:** THV minimum and maximum diameters, and perimeter were 19.5 mm, 24 mm and 68.1 mm in systole, respectively, and 19.5 mm, 23.7 mm and 68.2 mm in diastole, respectively. The minimum diameter was larger in Evolut THV, especially in diastole

(systole median 19.6 mm vs. 18.9 mm,  $p = 0.073$ ; diastole median 19.9 mm vs. 18.8 mm,  $p = 0.032$ ). No significant differences were observed between the two platforms in terms of maximum diameter (systole,  $p = 0.249$ ; diastole,  $p = 0.241$ ) and perimeter (systole,  $p = 0.894$ ; diastole,  $p = 0.857$ ).

**c) Inflow:** THV minimum and maximum diameters, and perimeter were 19.4 mm, 24 mm and 67.7 mm in systole, respectively, and 19.3 mm, 24 mm and 67.9 mm in diastole, respectively. No differences were reported between the two THVs in systolic measurements of minimum ( $p = 0.155$ ) or maximum diameter ( $p = 0.435$ ), and perimeter ( $p = 0.851$ ). In diastole, the minimum diameter was larger in Evolut THV (19.6 mm vs. 18.9 mm,  $p = 0.033$ ), but maximum diameter ( $p = 0.262$ ) and perimeter ( $p = 0.897$ ) did not differ.

### **Study endpoints**

Bioprosthetic stent expansion was encountered at BLP (perimeter +0.25 mm) and VBR (perimeter +0.30 mm) levels but not at the THV inflow (perimeter -0.05 mm).

Stent expansion was significantly greater in ACURATE compared to Evolut THV either at BLP (perimeter +0.60 mm vs. +0.20 mm,  $p = 0.050$ ) and VBR (perimeter +0.50 mm vs. +0.10 mm,  $p = 0.016$ ) levels, whereas no differences were reported at the inflow level (perimeter +0.10 mm vs. -0.30 mm,  $p = 0.192$ ) (**Table 20**).

**Table 19.** Transcatheter heart valve frame dimensions assessment at computed tomography angiography systolic and diastolic acquisitions. Data are presented as median mm [IQR]. VBR: Virtual basal ring.

		<b>Overall (n=83)</b>	<b>Evolut (n=49)</b>	<b>ACURATE (n=34)</b>	<b>p-val</b>
<b>Bioprosthetic leaflet plane</b>					
<b>Systole</b>	Min diameter	19.3 [18.1–20.6]	19.8 [18.9–20.7]	18.2 [17.1–20.0]	0.012
	Max diameter	23.5 [22.7–24.3]	23.4 [22.9–24.0]	23.6 [22.4–25.0]	0.650
	Perimeter	67.3 [64.9–69.6]	67.5 [66.1–69.4]	66.3 [62.9–70.0]	0.441
<b>Diastole</b>	Min diameter	19.6 [17.9–20.5]	19.9 [19.1–20.7]	18.2 [17.1–20.3]	0.008
	Max diameter	23.4 [22.4–23.9]	23.5 [22.8–23.8]	23.3 [22.1–24.9]	0.915
	Perimeter	67.5 [64.1–69.6]	67.8 [65.8–69.2]	64.3 [62.2–69.6]	0.234
<b>VBR</b>					
<b>Systole</b>	Min diameter	19.5 [18.4–20.6]	19.6 [18.6–21.1]	18.9 [18.0–20.0]	0.073
	Max diameter	24.0 [22.8–25.3]	23.8 [22.4–25.1]	24.2 [23.4–25.6]	0.249
	Perimeter	68.1 [64.8–72.1]	67.6 [64.8–71.7]	69.1 [64.9–73.0]	0.894
<b>Diastole</b>	Min diameter	19.5 [18.5–20.7]	19.9 [18.8–21.2]	18.8 [18.3–19.9]	0.032
	Max diameter	23.7 [22.6–25.2]	23.4 [22.4–25.1]	23.9 [23.1–25.5]	0.241
	Perimeter	68.2 [64.4–71.6]	68.3 [64.5–71.8]	68.0 [64.4–71.6]	0.857
<b>Inflow</b>					
<b>Systole</b>	Min diameter	19.4 [18.2–20.9]	19.6 [18.4–21.6]	19.0 [17.6–20.2]	0.155
	Max diameter	24.0 [22.9–25.7]	23.8 [22.4–25.7]	24.0 [23.0–25.7]	0.435
	Perimeter	67.7 [64.8–73.0]	67.4 [65.0–73.1]	69.1 [64.6–72.6]	0.851
<b>Diastole</b>	Min diameter	19.3 [18.1–20.5]	19.6 [18.8–21.7]	18.9 [17.5–19.7]	0.033
	Max diameter	24.0 [22.8–25.5]	23.8 [22.1–25.6]	24.1 [23.2–25.2]	0.262
	Perimeter	67.9 [64.8–73.0]	67.7 [65.2–74.0]	67.9 [64.7–72.6]	0.897

**Table 20.** Transcatheter heart valve stent expansion across cardiac the cycle. Data are presented as median mm [IQR]. VBR: Virtual basal ring.

	<b>Overall (n=83)</b>	<b>Evolut (n=49)</b>	<b>ACURATE (n=34)</b>	<b>p-val</b>
<b>Bioprosthetic leaflet plane</b>				
Min diameter	0.00 [-0.30, 0.40]	0.00 [-0.40, 0.30]	0.00 [-0.20, 0.40]	0.290
Max diameter	0.30 [-0.02, 0.60]	0.20 [-0.15, 0.55]	0.40 [0.00, 0.80]	0.063
Perimeter	0.25 [-0.52, 1.22]	0.20 [-0.60, 0.70]	0.60 [-0.30, 1.80]	<b>0.050</b>
<b>VBR</b>				
Min diameter	-0.10 [-0.43, 0.30]	-0.20 [-0.50, 0.15]	0.00 [-0.30, 0.40]	0.132
Max diameter	0.20 [-0.10, 0.50]	0.20 [-0.15, 0.55]	0.20 [-0.10, 0.40]	0.704
Perimeter	0.30 [-0.70, 0.80]	0.10 [-0.75, 0.45]	0.50 [-0.20, 1.00]	<b>0.016</b>
<b>Inflow</b>				
Min diameter	-0.15 [-0.60, 0.23]	-0.10 [-0.55, 0.15]	-0.20 [-0.60, 0.30]	0.494
Max diameter	0.10 [-0.30, 0.43]	0.20 [-0.25, 0.55]	-0.10 [-0.30, 0.20]	0.204
Perimeter	-0.05 [-0.82, 0.55]	-0.30 [-0.85, 0.25]	0.10 [-0.60, 1.10]	0.192

In the overall cohort, HALT was detected in 21.7% of patients, with numerically higher rates in Evolut recipients (24.5% vs. 17.6%;  $p = 0.591$ ; Table 6). Most cases were Grade 1, and only a single patient exhibited Grade 2 HALT. Bioprosthetic leaflets analysis showed that the right coronary cusp was the most involved (15.7%), followed by non-coronary (9.6%) and left (8.4%) cusps. No differences in HALT localization were reported between study devices (**Table 21**).

Finally, no cases of reduced leaflet motion (RLM) were observed.

**Table 21.** Incidence and characteristics of HALT and RLM after transcatheter aortic valve implantation. Data are presented as n (%). HALT: hypoattenuated leaflet thickening; RLM: restricted leaflet motion; RCC: right coronary cusp; LCC: left coronary cusp; NCC: non-coronary cusp.

		<b>Overall (n=83)</b>	<b>Evolut (n=49)</b>	<b>ACURATE (n=34)</b>	<b>p-val</b>
<b>HALT</b>	<i>Overall</i>	18 (21.7%)	12 (24.5%)	6 (17.6%)	0.591
	<b>Grades</b>				
	<i>Grade 1</i>	17 (20.5%)	11 (22.4%)	6 (17.6%)	
	<i>Grade 2</i>	1 (1.2%)	1 (2.0%)	0 (0.0%)	
	<i>Grade 3</i>	0 (0.0)	0 (0.0)	0 (0.0)	
	<b>Localization</b>				
	<i>RCC</i>	13 (15.7%)	8 (16.3%)	5 (14.7%)	
	<i>LCC</i>	7 (8.4%)	3 (6.1%)	4 (11.8%)	
	<i>NCC</i>	8 (9.6%)	7 (14.3%)	1 (2.9%)	
<b>RLM</b>		0 (0.0%)	0 (0.0%)	0 (0.0%)	-

### Predictors of THV frame expansion

Univariable and multivariable linear regression analyses investigating procedure-related factors associated with THV frame expansion were reported in **Table 22**.

At multivariable logistic regression analysis, the use of ACURATE neo2 THV (OR 0.23; 95% CI 0.02-0.92; p=0.041) and severe leaflets calcifications (OR 0.29; 95% CI 0.14-1.14; p=0.014) were the only factors independently associated with THV frame expansion.

**Table 22.** Univariable and multivariable linear regression analyses investigating procedure-related factors associated with transcatheter heart valve (THV) frame expansion. Data are presented as Odds Ratio (OR) with 95% confidence intervals (CI).

	<b>Univariable [OR (95% CI)]</b>	<b>p-val</b>	<b>Multivariable [OR (95% CI)]</b>	<b>p-val</b>
ACURATE neo2 THV	0.27 (0.07;1.00)	0.024	0.23 (0.02;0.92)	0.041
Post-dilatation	0.08 (-0.48;0.96)	0.512		
Severe leaflets calcifications	0.31 (0.19;1.20)	0.008	0.29 (0.14;1.14)	0.014
Severe THV misalignment	0.69 (-0.56;1.02)	0.566		
THV oversizing	-0.25 (-0.06;0.00)	0.035		
ACURATE THV under-expansion	0.69 (-1.89;2.68)	0.723		

#### **4.4 Discussion**

The progressive expansion of TAVR to younger and lower-risk patients has intensified concerns regarding prosthesis durability and long-term clinical outcomes. In this context, the biomechanical interaction between THVs frames and the native aortic root has emerged as a critical determinant of valve function, influencing leaflet motion, flow patterns, and the pathogenesis of HALT and RLM (51,52).

In the native aortic valve, the dynamic coupling between leaflets and root ensures optimal hemodynamics and minimizes leaflet stress. The introduction of a prosthetic frame can disrupt this physiological and synchronous interplay, potentially impairing root motion and promoting regions of flow stagnation. Among THVs, nitinol-based SE platforms may offer an advantage compared to balloon-expandable THVs, theoretically transmitting the native excursions of the aortic annulus to the bioprosthetic leaflets.

Despite sharing a self-expanding design with supra-annular leaflet positioning, ACURATE and Evolut platforms markedly differ in their structural architecture, radial force, and deployment mechanism. These differences may translate into different biomechanical behaviour, which in turn may theoretically impact valve hemodynamic (53,54).

A bench-top model simulating physiological flow conditions was used to compare four TAVR platforms (ACURATE neo, Evolut R, Allegra, and SAPIEN 3). Open-frame, supra-annular valves (ACURATE and Evolut) demonstrated faster washout and higher shear stress—features typically associated with reduced flow stasis and lower thrombogenicity. However, these same valves also exhibited greater leaflet flutter and elevated turbulence levels, which may increase mechanical blood trauma and potentially offset their hemodynamic benefits in certain anatomical settings (55,56). These apparently conflicting data highlight the complex and multifactorial relationship between frame design, leaflet motion, and flow behaviour, shaped by anatomical, procedural, and structural variables.

In this analysis, we explored for the first time the in-vivo behaviour of Evolut and ACURATE Neo2 THV platforms across the cardiac cycle. Both platforms showed perimeter expansion in systole at BLP and VBR level but not at the inflow edge.

The ACURATE neo2 demonstrated higher dynamicity of the frame across the cardiac cycle, with a significantly greater perimeter expansion at BLP and VBR levels, consistent with increased adaptive compliance to aortic root physiology. This finding was further supported by regression analysis, which identified the ACURATE neo2 device as an independent predictor of THV frame expansion.

Recently, a post-hoc analysis of the ACURATE IDE trial found that a significant THV under-expansion was encountered in ~20% of ACURATE neo2 patients, and it was independently associated with impaired hemodynamic and adverse outcomes (57).

Similarly, Won-Keun Kim et al. reported that under-expanded ACURATE valves exhibited incomplete leaflet opening, elevated gradients, and altered flow promoting HALT development (58).

While frame under-expansion has been proposed to disturb valve functioning and blood flow, we observed numerically lower - but not statistically significant - rates of HALT with ACURATE THV. In our study, we reported a single case of ACURATE THV untreated under-expansion (2.9% of ACURATE THVs). This finding may generate the hypothesis that, when ACURATE THV is well expanded, its frame compliance and cyclical adaptability may exert a protective effect by maintaining more physiological flow.

Unlike the tight-cell frame of Evolut THV, the ACURATE frame is lighter, with a more open-cell design and notably lacks a metallic scaffold directly behind the leaflets—features that may facilitate greater root interaction and reduce local flow stagnation.

Notably, our findings should be interpreted as exploratory due to the relatively small sample size and the limited statistical power of our sub-analysis. Larger studies are needed

to confirm these trends and clarify the mechanistic links between frame dynamics and HALT/valve deterioration.

Within this evolving field, next-generation biomimetic platforms such as DurAVR represent a promising innovation. By leveraging ultra-compliant frames and anatomical leaflet geometry, these devices aim to restore native aortic root physiology and optimize flow patterns. Early-phase CMR data suggest favourable restoration of laminar flow and systolic flow reversal—features often disrupted following both TAVR and SAVR (59).

Although the ACURATE platform has now been withdrawn from the market, our findings provide meaningful insights into how THV biomechanics affect leaflet function and flow.

These insights remain highly relevant as valve therapy continues to expand to younger populations, for whom durability and thrombotic risk are of paramount importance.

Future research integrating imaging, fluid dynamics, and long-term clinical outcomes will be critical to guide next-generation valve design and improve the durability profile of TAVR.

#### **4.5 Limitations**

Different limitations should be acknowledged. Despite the presence of an independent CTA core laboratory assessment, the relatively small sample size, single-centre, non-randomized design, and cross-sectional assessment limit generalizability and preclude evaluation of longitudinal changes. Results should therefore be considered exploratory and hypothesis-generating, warranting validation in larger, multicenter studies with long-term follow-up.

## 5. CONCLUSIONS

The investigator-initiated REACCESS 2 (Reobtain Coronary Ostia Cannulation Beyond Transcatheter Aortic Valve Stent 2) study was the first, prospective trial to evaluate TAVR outcomes in patients receiving the self-expanding Evolut or ACURATE Neo2 THVs with intentional, patient-specific commissural alignment (CA). Unsuccessful coronary cannulation following TAVR using self-expanding, supra-annular THVs implanted with CA technique was reported in 5.5% of cases, with the majority involving the Evolut THV platform. The right coronary artery cannulation confirmed to pose the most significant challenge. Importantly, systematic CA notably improved coronary re-access capability, especially among patients receiving Evolut THV. Nevertheless, a severe misalignment mostly impacted coronary cannulation after TAVR in these patients.

At post-TAVR 4D-CTA analysis, SE, nitinol-based THVs showed frame expansion at bioprosthetic leaflet plane (BLP) and virtual basal ring (VBR) level. The ACURATE Neo2 platform showed a significantly greater stent expansion at those levels, and a numerically lower hypo-attenuated leaflet thickening (HALT) rates. These findings highlight that the in-vivo biomechanical interplay between frame design and native root dynamics may impact flow behaviour, which in turn might affect leaflets structural integrity. A clearer understanding of these mechanisms is essential to guide future developments and to improve TAVR outcomes. Next-generation THV development should prioritize restoring native biomechanics, minimizing thrombotic risk, and achieving durable clinical outcomes beyond procedural success.

## 6. REFERENCES

1. Otto CM., Nishimura RA., Bonow RO., et al. 2020 ACC/AHA Guideline for the Management of Patients With Valvular Heart Disease: A Report of the American College of Cardiology/American Heart Association Joint Committee on Clinical Practice Guidelines. *Circulation* 2021;143(5). Doi: 10.1161/CIR.0000000000000923.
2. Praz F., Borger MA., Lanz J., et al. 2025 ESC/EACTS Guidelines for the management of valvular heart disease. *Eur Heart J* 2025. Doi: 10.1093/eurheartj/ehaf194.
3. Yudi MB., Sharma SK., Tang GHL., Kini A. Coronary Angiography and Percutaneous Coronary Intervention After Transcatheter Aortic Valve Replacement. *J Am Coll Cardiol* 2018;71(12):1360–78. Doi: 10.1016/j.jacc.2018.01.057.
4. Fuchs A., Kofoed KF., Yoon S-H., et al. Commissural Alignment of Bioprosthetic Aortic Valve and Native Aortic Valve Following Surgical and Transcatheter Aortic Valve Replacement and its Impact on Valvular Function and Coronary Filling. *JACC Cardiovasc Interv* 2018;11(17):1733–43. Doi: 10.1016/j.jcin.2018.05.043.
5. Barbanti M., Costa G., Picci A., et al. Coronary Cannulation After Transcatheter Aortic Valve Replacement. *JACC Cardiovasc Interv* 2020;13(21):2542–55. Doi: 10.1016/j.jcin.2020.07.006.
6. Valvo R., Costa G., Tamburino C., Barbanti M. Coronary artery cannulation after transcatheter aortic valve implantation. *EuroIntervention* 2021;17(10):835–47. Doi: 10.4244/EIJ-D-21-00158.
7. Tarantini G., Nai Fovino L., Le Prince P., et al. Coronary Access and Percutaneous Coronary Intervention Up to 3 Years After Transcatheter Aortic Valve Implantation With a Balloon-Expandable Valve. *Circ Cardiovasc Interv* 2020;13(7). Doi: 10.1161/CIRCINTERVENTIONS.120.008972.

8. Nai Fovino L., Scotti A., Massussi M., et al. Incidence and feasibility of coronary access after transcatheter aortic valve replacement. *Catheterization and Cardiovascular Interventions* 2020;96(5):E535–41. Doi: 10.1002/ccd.28720.
9. Ochiai T., Chakravarty T., Yoon S-H., et al. Coronary Access After TAVR. *JACC Cardiovasc Interv* 2020;13(6):693–705. Doi: 10.1016/j.jcin.2020.01.216.
10. Rogers T., Greenspun BC., Weissman G., et al. Feasibility of Coronary Access and Aortic Valve Reintervention in Low-Risk TAVR Patients. *JACC Cardiovasc Interv* 2020;13(6):726–35. Doi: 10.1016/j.jcin.2020.01.202.
11. Tarantini G., Nai Fovino L., Scotti A., et al. Coronary Access After Transcatheter Aortic Valve Replacement With Commissural Alignment: The ALIGN-ACCESS Study. *Circ Cardiovasc Interv* 2022;15(2). Doi: 10.1161/CIRCINTERVENTIONS.121.011045.
12. Arshi A., Yakubov SJ., Stiver KL., Sanchez CE. Overcoming the transcatheter aortic valve replacement Achilles heel: coronary re-access. *Ann Cardiothorac Surg* 2020;9(6):468–77. Doi: 10.21037/acs-2020-av-38.
13. Salmonsmith JA., Ducci A., Burriesci G. Does transcatheter aortic valve alignment matter? *Open Heart* 2019;6(2):e001132. Doi: 10.1136/openhrt-2019-001132.
14. Hatoum H., Dollery J., Lilly SM., Crestanello JA., Dasi LP. Implantation Depth and Rotational Orientation Effect on Valve-in-Valve Hemodynamics and Sinus Flow. *Ann Thorac Surg* 2018;106(1):70–8. Doi: 10.1016/j.athoracsur.2018.01.070.
15. Khan JM., Rogers T., Weissman G., et al. Anatomical Characteristics Associated With Hypoattenuated Leaflet Thickening in Low-Risk Patients Undergoing Transcatheter Aortic Valve Replacement. *Cardiovascular Revascularization Medicine* 2021;27:1–6. Doi: 10.1016/j.carrev.2020.09.034.
16. Raschpichler M., Flint N., Yoon S-H., et al. Commissural Alignment After Balloon-Expandable Transcatheter Aortic Valve Replacement Is Associated With Improved

- Hemodynamic Outcomes. *JACC Cardiovasc Interv* 2022;15(11):1126–36. Doi: 10.1016/j.jcin.2022.04.006.
17. Greenbaum AB., Kamioka N., Vavalle JP., et al. Balloon-Assisted BASILICA to Facilitate Redo TAVR. *JACC Cardiovasc Interv* 2021;14(5):578–80. Doi: 10.1016/j.jcin.2020.10.056.
  18. Khan JM., Babaliaros VC., Greenbaum AB., et al. Preventing Coronary Obstruction During Transcatheter Aortic Valve Replacement. *JACC Cardiovasc Interv* 2021;14(9):941–8. Doi: 10.1016/j.jcin.2021.02.035.
  19. Tang GHL., Zaid S. Coronary re-access after redo TAVI: a proposed classification to simplify evaluation. *EuroIntervention* 2020;16(12):e960–2. Doi: 10.4244/EIJV16I12A176.
  20. De Backer O., Landes U., Fuchs A., et al. Coronary Access After TAVR-in-TAVR as Evaluated by Multidetector Computed Tomography. *JACC Cardiovasc Interv* 2020;13(21):2528–38. Doi: 10.1016/j.jcin.2020.06.016.
  21. Fovino LN., Scotti A., Massussi M., et al. Coronary angiography after transcatheter aortic valve replacement (TAVR) to evaluate the risk of coronary access impairment after tavr-in-tavr. *J Am Heart Assoc* 2020;9(13):1–18. Doi: 10.1161/JAHA.120.016446.
  22. Tarantini G., Fabris T., Nai Fovino L. TAVR-in-TAVR and coronary access: importance of preprocedural planning. *EuroIntervention* 2020;16(2):e129–32. Doi: 10.4244/EIJ-D-19-01094.
  23. Buzzatti N., Montorfano M., Romano V., et al. A computed tomography study of coronary access and coronary obstruction after redo transcatheter aortic valve implantation. *EuroIntervention* 2020;16(12):e1005–13. Doi: 10.4244/EIJ-D-20-00475.

24. Tarantini G., Dvir D., Tang GHL. Transcatheter aortic valve implantation in degenerated surgical aortic valves. *EuroIntervention* 2021;17(9):709–19. Doi: 10.4244/EIJ-D-21-00157.
25. Tang GHL., Amat-Santos IJ., De Backer O., et al. Rationale, Definitions, Techniques, and Outcomes of Commissural Alignment in TAVR. *JACC Cardiovasc Interv* 2022;15(15):1497–518. Doi: 10.1016/j.jcin.2022.06.001.
26. Bieliauskas G., Wong I., Bajoras V., et al. Patient-Specific Implantation Technique to Obtain Neo-Commissural Alignment With Self-Expanding Transcatheter Aortic Valves. *JACC Cardiovasc Interv* 2021;14(19):2097–108. Doi: 10.1016/j.jcin.2021.06.033.
27. Redondo A., Valencia-Serrano F., Santos-Martínez S., et al. Accurate commissural alignment during ACURATE neo TAVI procedure. Proof of concept. *Rev Esp Cardiol* 2021. Doi: 10.1016/j.recesp.2021.02.008.
28. Tang GHL., Zaid S., Fuchs A., et al. Alignment of Transcatheter Aortic-Valve Neo-Commissures (ALIGN TAVR): Impact on Final Valve Orientation and Coronary Artery Overlap. *JACC Cardiovasc Interv* 2020;13(9):1030–42. Doi: 10.1016/j.jcin.2020.02.005.
29. Tang GHL., Zaid S., Gupta E., et al. Impact of Initial Evolut Transcatheter Aortic Valve Replacement Deployment Orientation on Final Valve Orientation and Coronary Reaccess. *Circ Cardiovasc Interv* 2019;12(7). Doi: 10.1161/CIRCINTERVENTIONS.119.008044.
30. Tang GHL., Sengupta A., Alexis SL., et al. Conventional versus modified delivery system technique in commissural alignment from the Evolut <sc>low-risk CT substudy</sc>. *Catheterization and Cardiovascular Interventions* 2022;99(3):924–31. Doi: 10.1002/ccd.29973.

31. Redondo A., Santos-Martínez S., Delgado-Arana R., Baladrón Zorita C., San Román JA., Amat-Santos IJ. Fluoroscopic-based algorithm for commissural alignment assessment after transcatheter aortic valve implantation. *Revista Española de Cardiología (English Edition)* 2022;75(2):184–7. Doi: 10.1016/j.rec.2021.08.010.
32. Faroux L., Munoz-Garcia E., Serra V., et al. Acute Coronary Syndrome Following Transcatheter Aortic Valve Replacement. *Circ Cardiovasc Interv* 2020;13(2). Doi: 10.1161/CIRCINTERVENTIONS.119.008620.
33. Faroux L., Lhermusier T., Vincent F., et al. ST-Segment Elevation Myocardial Infarction Following Transcatheter Aortic Valve Replacement. *J Am Coll Cardiol* 2021;77(17):2187–99. Doi: 10.1016/j.jacc.2021.03.014.
34. Barbanti M., Todaro D., Costa G., et al. Optimized Screening of Coronary Artery Disease With Invasive Coronary Angiography and Ad Hoc Percutaneous Coronary Intervention During Transcatheter Aortic Valve Replacement. *Circ Cardiovasc Interv* 2017;10(8). Doi: 10.1161/CIRCINTERVENTIONS.117.005234.
35. Chen F., Xiong T., Li Y., et al. Risk of Coronary Obstruction During Redo-TAVR in Patients With Bicuspid Versus Tricuspid Aortic Valve Stenosis. *JACC Cardiovasc Interv* 2022;15(7):712–24. Doi: 10.1016/j.jcin.2022.01.282.
36. Génèreux P., Piazza N., Alu MC., et al. Valve Academic Research Consortium 3: updated endpoint definitions for aortic valve clinical research. *Eur Heart J* 2021;42(19):1825–57. Doi: 10.1093/eurheartj/ehaa799.
37. Thyregod HGH., Ihlemann N., Jørgensen TH., et al. Five-Year Clinical and Echocardiographic Outcomes From the NOTION Randomized Clinical Trial in Patients at Lower Surgical Risk. *Circulation* 2019;139(24):2714–23. Doi: 10.1161/CIRCULATIONAHA.118.036606.
38. Pibarot P., Salaun E., Dahou A., et al. Echocardiographic Results of Transcatheter Versus Surgical Aortic Valve Replacement in Low-Risk Patients: The PARTNER 3

Trial. *Circulation* 2020;CIRCULATIONAHA.119.044574. Doi: 10.1161/CIRCULATIONAHA.119.044574.

39. Popma JJ., Michael Deeb G., Yakubov SJ., et al. Transcatheter aortic-valve replacement with a self-expanding valve in low-risk patients. *New England Journal of Medicine* 2019;380(18):1706–15.
40. Mack MJ., Leon MB., Thourani VH., et al. Transcatheter Aortic-Valve Replacement in Low-Risk Patients at Five Years. *New England Journal of Medicine* 2023;389(21):1949–60. Doi: 10.1056/NEJMoa2307447.
41. Mack MJ., Leon MB., Thourani VH., et al. Transcatheter Aortic-Valve Replacement with a Balloon-Expandable Valve in Low-Risk Patients. *New England Journal of Medicine* 2019;380(18):1695–705.
42. Leon MB., Smith CR., Mack MJ., et al. Transcatheter or Surgical Aortic-Valve Replacement in Intermediate-Risk Patients. *N Engl J Med* 2016;374(17):1609–20.
43. Reardon MJ., Van Mieghem NM., Popma JJ., et al. Surgical or Transcatheter Aortic-Valve Replacement in Intermediate-Risk Patients. *N Engl J Med* 2017;376(14):1321–31.
44. Barbanti M., Tamburino C. Late degeneration of transcatheter aortic valves: pathogenesis and management. *EuroIntervention* 2016;12(Y):Y33–6. Doi: 10.4244/EIJV12SYA8.
45. Costa G., Criscione E., Todaro D., Tamburino C., Barbanti M. Long-term Transcatheter Aortic Valve Durability. *Interventional Cardiology Review* 2019;14(2):62–9. Doi: 10.15420/icr.2019.4.2.
46. Ncho B., Sadri V., Ortner J., Kollapaneni S., Yoganathan A. In-Vitro Assessment of the Effects of Transcatheter Aortic Valve Leaflet Design on Neo-Sinus Geometry and Flow. *Ann Biomed Eng* 2021;49(3):1046–57. Doi: 10.1007/s10439-020-02664-0.

47. Hatoum H., Dollery J., Lilly SM., Crestanello J., Dasi LP. Impact of patient-specific morphologies on sinus flow stasis in transcatheter aortic valve replacement: An in vitro study. *J Thorac Cardiovasc Surg* 2019;157(2):540–9. Doi: 10.1016/j.jtcvs.2018.05.086.
48. Hatoum H., Yousefi A., Lilly S., Maureira P., Crestanello J., Dasi LP. An in vitro evaluation of turbulence after transcatheter aortic valve implantation. *J Thorac Cardiovasc Surg* 2018;156(5):1837–48. Doi: 10.1016/j.jtcvs.2018.05.042.
49. Liu X., Zhang W., Ye P., Luo Q., Chang Z. Fluid-Structure Interaction Analysis on the Influence of the Aortic Valve Stent Leaflet Structure in Hemodynamics. *Front Physiol* 2022;13. Doi: 10.3389/fphys.2022.904453.
50. Costa G., Sammartino S., Strazzieri O., et al. Coronary Cannulation Following TAVR Using Self-Expanding Devices With Commissural Alignment. *JACC Cardiovasc Interv* 2024;17(6):727–37. Doi: 10.1016/j.jcin.2023.12.015.
51. Forrest JK., Yakubov SJ., Deeb GM., et al. 5-Year Outcomes After Transcatheter or Surgical Aortic Valve Replacement in Low-Risk Patients With Aortic Stenosis. *J Am Coll Cardiol* 2025;85(15):1523–32. Doi: 10.1016/j.jacc.2025.03.004.
52. Makkar RR., Blanke P., Leipsic J., et al. Subclinical Leaflet Thrombosis in Transcatheter and Surgical Bioprosthetic Valves. *J Am Coll Cardiol* 2020;75(24):3003–15. Doi: 10.1016/j.jacc.2020.04.043.
53. Baggio S., Pagnesi M., Kim W-K., et al. Comparison of transcatheter aortic valve replacement with the ACURATE neo2 versus Evolut PRO/PRO+ devices. *EuroIntervention* 2023;18(12):977–86. Doi: 10.4244/EIJ-D-22-00498.
54. Tamburino C., Bleiziffer S., Thiele H., et al. Comparison of Self-Expanding Bioprostheses for Transcatheter Aortic Valve Replacement in Patients With Symptomatic Severe Aortic Stenosis. *Circulation* 2020;142(25):2431–42. Doi: 10.1161/CIRCULATIONAHA.120.051547.

55. Hatoum H., Samaee M., Sathananthan J., et al. Comparison of performance of self-expanding and balloon-expandable transcatheter aortic valves. *JTCVS Open* 2022;10:128–39. Doi: 10.1016/j.xjon.2022.04.015.
56. Hatoum H., Gooden SCM., Sathananthan J., et al. Neosinus and Sinus Flow After Self-Expanding and Balloon-Expandable Transcatheter Aortic Valve Replacement. *JACC Cardiovasc Interv* 2021;14(24):2657–66. Doi: 10.1016/j.jcin.2021.09.013.
57. Makkar RR., Chakravarty T., Gupta A., et al. Valve Underexpansion and Clinical Outcomes With ACURATE neo2. *J Am Coll Cardiol* 2025;86(4):225–38. Doi: 10.1016/j.jacc.2025.05.011.
58. Kim W-K., de Backer O., Renker M., et al. Clinical Impact of Midframe Underexpansion Following TAVR Using a Self-Expanding Transcatheter Heart Valve. *JACC Cardiovasc Interv* 2025;18(8):1028–41. Doi: 10.1016/j.jcin.2025.02.013.
59. Kodali SK., Sorajja P., Meduri CU., et al. Early safety and feasibility of a first-in-class biomimetic transcatheter aortic valve - DurAVR. *EuroIntervention* 2023;19(4):e352–62. Doi: 10.4244/EIJ-D-23-00282.